Three-Dimensional Visualization of Oxygen Distribution in Wastewater Biofilm

by

Zi'ang Zhu

A thesis submitted in partial fulfillment of the requirements for the degree of

Master of Science

in

Environmental Science

Department of Civil and Environmental Engineering

University of Alberta

Abstract

Three-dimensional (3-D) visualization of the distribution of chemical species of interest in biofilms enhances our understanding of important structural and functional characteristics of biofilms. In a previous study, the 3-D oxygen distribution in an approximately 1 mm^3 wastewater biofilm was mapped by using oxygen microsensor. However, there has been a lack of method for effective visualization of 3-D oxygen distribution in biofilms. This study developed a Matlab package for 3-D visualization of oxygen distribution in wastewater biofilm as well as on and near biofilm surface. In the package, colormap slices, contour slices, isosurfaces, and animations were used for the visualization. It was found that the oxygen pockets in deep sections of biofilm existed in isolation, which indicates that the biofilm is physiologically heterogeneous. The oxygen concentration on the biofilm surface was observed to be much lower than that of bulk liquid phase, indicating a high intensity of metabolic activity in biofilm. The interception line between biofilm surface and horizontal slice was clearly visualized, which is helpful for comparing the vertical distribution of bacteria biovolume along the biofilm depth. The visualization method in this study will greatly help researchers to understand the 3-D heterogeneity of biofilms, and to gain more insight for the structural and functional features of wastewater biofilms. This Matlab package developed in this study can also support 3-D visualization of other chemical species of interest in biofilms where data are available.

Acknowledgements

Firstly, I would like to express my deepest gratitude to my research supervisor, Dr. Tong Yu, whose patience, encouragement and stimulating suggestions helped me throughout my master study, shaping my interest in environmental engineering and at the same time helping to form my appreciation of scientific research.

In addition, I would like to thank Dr. Ian Buchanan and Dr. William Wenming Zhang for serving in my thesis defense committee, and for their insightful suggestions and comments on my study. I would like to thank Dr. Yu's group members: Lei Zhu, Yijun Chen, Hannah Kratky, Zhan Li. It is wonderful to have all of you around to help me find answers to questions that confused me. Many thanks to my friends who made my life at the University of Alberta very enjoyable and energetic

Moreover, I would like to thank my parents for their unwavering support and enthusiasm throughout my master study. I would also like to acknowledge financial support from the Natural Science and Engineering Research Council (NSERC) grant.

Table of Content

List of Figures

List of Table

1 Introduction

1.1 Background

Biofilm processes have been widely used for the treatment of municipal and industrial wastewater. A correct understanding of the complex structural and functional characteristics of biofilms is essential for the optimal design and operation of biofilm processes (Lewandowski & Beyenal, 2013). Oxygen is an important biofilm chemical species which is used as the final electron acceptor in aerobic biodegradation. The distribution of oxygen often defines the structures and functions of biofilms. A reliable tool to measure oxygen distribution in biofilms is oxygen microsensors. Due to the heterogeneity of biofilms, the three-dimensional (3-D) mapping of oxygen carries significant information regarding biofilm structures and functions that can hardly be seen in typical one-dimensional (1-D) oxygen profiles (de la Rosa & Yu, 2005). Using an automation system and oxygen microsensor, de la Rosa and Yu (2005) obtained the first data sets of 3-D distribution of oxygen in wastewater biofilms with thickness around 1000 μm. The data obtained from this study are helpful for the validation of two-dimensional (2-D) and 3-D biofilm models (Noguera et al., 1999; Eberl et al., 2000; Morgenroth 2000a, 2000b) that evaluate the 3-D heterogeneity of oxygen distribution.

Another important technique for analyzing biofilm 3-D heterogeneity is confocal scanning laser microscopy (CLSM). The user of CLSM can obtain sequential 2-D optical images about biomass distribution by changing the depths of the focal plane once a time. The sequential CLSM images can be stacked using appropriate software to reconstruct 3-D structure of biofilms. However, there is a penetration depth of CLSM which limits the detection depth within biofilms when using CLSM analysis. The working distance between

the lens and the object imposes an upper limit of penetration depth (Morgan *et al*., 2013). The penetration depth is further limited when the sample absorbs excitation photons or scatters both the excitation and emission photons (Morgan *et al*., 2013). Even under optimized conditions, the effective penetration depth of CLSM analysis is 100 μm depending on the nature of samples (Reihani & Oddershede, 2009; Morgan *et al*., 2013). Considering the fact that the thickness of most mature wastewater biofilms is in the range of 500-2000 μm (Bishop, 1997), CLSM analysis cannot effectively evaluate 3-D heterogeneity in deep sections of thick wastewater biofilms.

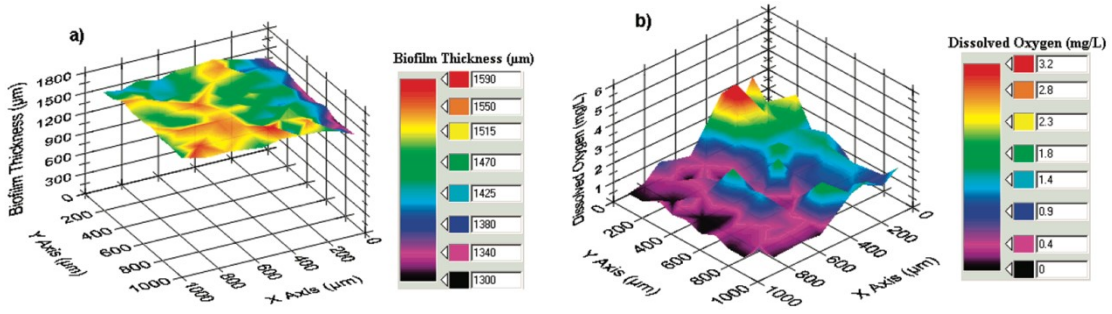

Fig 1-1 Physical structure and oxygen distribution on biofilm surface

a) Physical structure of biofilm surface b) Oxygen distribution on biofilm surface. The heights of peaks represent the concentrations of oxygen instead of the morphology of biofilm surface. (de la Rosa & Yu, 2005)

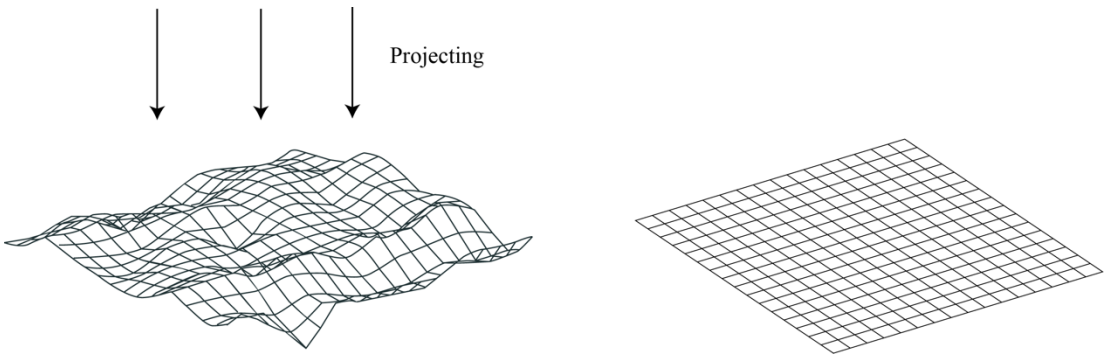

Fig 1-2 Projecting an irregular surface onto a plane

The knowledge generated by the previous study on 3-D oxygen distribution provided a complete picture about the 3-D heterogeneity in thick wastewater biofilms. The authors reported a descending heterogeneity of oxygen distribution from the surface sections of biofilms to deep sections of biofilms, and the existence of 'oxygen pockets' in deep sections of biofilms. The authors also determined the thicknesses and surface structures of biofilm samples using oxygen microsensor. However, there is a lack of effective method for the presentation of 3-D heterogeneity of oxygen distribution in biofilms. There are two flaws in the way that the 3-D oxygen distribution data were presented. Firstly, the oxygen distribution on each 'cross section' was presented individually (e.g. Fig 1-1 (b), Fig 1-3 (a), and Fig 1-3 (b)) instead of being presented three-dimensionally, resulting in a loss of 3-D oxygen heterogeneity details. This method of presentation will require readers' spatial imagination to pile up these 'cross sections' together in order to better understand the 3-D oxygen distribution inside biofilms. Secondly, when the oxygen distribution on the biofilm surface and on individual surfaces that are parallel to biofilm surface was presented, the morphology of these irregular surfaces was ignored. For example, Fig 1-1 (b) shows the oxygen distribution on a biofilm surface, and the heights of peaks in Fig 1-1 (b) was used to represent oxygen concentrations on the biofilm surface. Yet this way of presentation is 'projecting' the irregular biofilm surface onto a plane (Fig 1-2), because no information regarding biofilm surface morphology was presented in Fig 1-1 (b). Therefore, there is a pressing need to develop a method for the effective visualization of 3-D oxygen distribution in wastewater biofilm as well as on and near biofilm surface in order to help researchers gain more insight for the structural and functional features of biofilms.

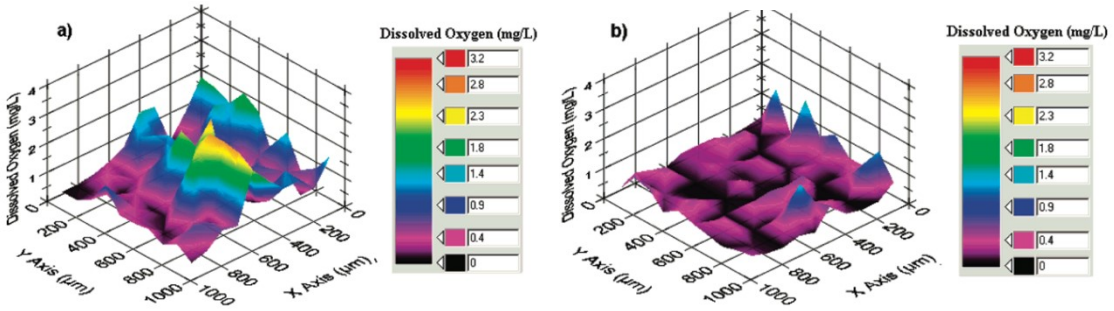

Fig 1-3 Oxygen distribution at different depths below biofilm surface

a): depth 40 µm b): depth 280 µm (de la Rosa & Yu, 2005).

1.2 Objectives

The objectives of this study are to (1) develop a method for effective 3-D visualization of oxygen distribution in wastewater biofilm as well as on and near biofilm surface and (2) use the visualization method to enhance our understanding on structural and functional characteristics of biofilm. The 3-D oxygen profile was determined by using oxygen microsensor in a previous study.

2 Literature review

This section firstly reviews significant contributions regarding the evaluation of biofilm structural and functional characteristics using oxygen microsensors. Next, it reviews the currently available techniques for 3-D reconstruction of biofilm structures.

2.1 Evaluating biofilm characteristics using oxygen microsensors

Microsensors are powerful tools in biofilm research. By using microsensors, researchers could accurately determine local chemical concentrations with high spatial resolution and with minimum disturbance on biofilm structure, obtaining information that is hard to be gathered otherwise (Lewandowski & Beyenal, 2013). The concentration profiles of different chemical species carry significant information about mass transport and microbial activity in biofilms. Oxygen microsensors are one of the most important microsensors because oxygen microsensors detect microscale levels of dissolved oxygen, which plays a crucial role in microbial activities. This section presents important contributions regarding the evaluation of biofilm characteristics using oxygen microsensors.

Zhang and Bishop (1995) investigated the thickness of oxygen concentration boundary layer and external mass transfer resistance in a wastewater biofilm system using oxygen microsensor. The authors reported that the thickness of oxygen concentration boundary layer was not in perfect agreement with theoretical predictions, because the fluctuations of oxygen velocity and concentration caused by the irregularity of biofilm surface would result in the compression of oxygen concentration boundary layer.

De Beer et al. (1994) assessed the relationship of biofilm internal structure and oxygen concentration profile using CLSM and oxygen microelectrode techniques. It was reported

that the aerobic biofilms have a highly heterogeneous structure, and the oxygen transfer was strongly influenced by the complex structure of biofilms. The oxygen concentration boundary layer was observed to follow the irregularities of biofilm surface instead of being parallel to the substratum. The authors suggested to develop a 3-D model to better calculation of mass transfer rates under different flow regimes.

Yu and Bishop (1998) examined the stratification of different microbial activities and the associated redox potential variation in an aerobic biofilm by using microsensors. It was demonstrated that oxygen was depleted at 550 μm below the surface, indicating the deeper sections of biofilm was anaerobic. It was also demonstrated that the sulfate reduction was active in deep anaerobic sections of the biofilm even the concentration of sulfate was low in the anaerobic sections. The findings from this study provided strong evidence for the concept that microbial metabolic activity was stratified in biofilms.

It is also important to evaluate the characteristics of biofilms which were directly sampled from full-scale wastewater treatment plants using oxygen microsensors. Most studies on oxygen transfer were conducted on laboratory-cultured biofilms (De Beer et al., 1994; Zhang & Bishop, 1995; Yu & Bishop, 1998; Satoh et al., 2005), while it is unknown whether the oxygen penetration in biofilms growing in wastewater treatment plants is different from the oxygen penetration in laboratory-cultured biofilms. Using microsensors, De Beer et al. (1997) measured the profiles of oxygen, nitrate, nitrite and hydrogen sulfide in a thick denitrifying biofilm sampled from the activated sludge basin of a municipal wastewater treatment plant. The oxygen penetration depth was reported to be less than 250 μm. Lu and Yu (2002) measured *in situ* oxygen transfer in biofilms from rotating biological contactors (RBC) operating in a municipal wastewater treatment plant. The authors reported oxygen penetration depths of no more than 600 μm in all biofilms studied, and

reported that the length of operation time appeared to influence the depth of oxygen penetration in biofilms. Therefore, studies on the oxygen transfer in biofilms from full-scale wastewater treatment systems greatly enhanced the understanding on the structural and functional characteristics of biofilms used in practical wastewater treatment.

The inhibitory effects of inhibitors on microbial activities can be effectively evaluated using microsensors. Using oxygen and ammonium microsensors, Satoh et al. (2005) investigated the temporal and spatial inhibitory effects of 2-chlorophenol (2-CP) on oxygen respiration and nitrification activity in wastewater biofilms. It was reported that 2-CP inhibited microbial activities within 6-18 minutes, and that microbial activities were inhibited only in the upper 400 μm of the biofilms by 2-CP. It was also reported the inhibitory ratios of 2-CP on oxygen respiration and nitrification activities are different: oxygen respiration was only incompletely inhibited, while nitrification was remarkably inhibited. Zhou et al. (2011) determined the temporal and spatial inhibitory effects of zinc and copper on the metabolic activity of wastewater biofilms based on inhibitory oxygen concentration profiles. The authors reported that that metabolic activities were inhibited only in the upper 400 μm of the biofilms, while metabolic activity in the deeper sections of biofilms was enhanced after the addition of zinc and copper inhibitors.

Zhou et al. (2012) calculated biokinetic parameters in wastewater biofilms using oxygen concentration profiles measured by microsensor. The authors measured several oxygen profiles in biofilm samples using microsensor, and then determined heterotrophic biokinetic parameters by fitting data to different diffusion-reaction models. The maintenance decay coefficient for oxygen (K_m), the Monod half saturation coefficient of oxygen (k_o), and the maximum specific oxygen uptake rate (q_{max}) in wastewater biofilms were quantified. The biokinetic parameters presented and evaluated in this study can be

imported into biofilm models that guide the optimization of design and operation of biofilm reactors.

Oxygen microsensors are often used in combination with other types of microsensors to study multiple microbial processes in biofilms. Tan et al. (2013) measured the profiles of different chemical species in a piece of membrane aerated biofilm (MAB) using O_2, H_2S, pH, ORP, NH_4^+ and NO_3^- microsensors. High oxygen consumption rate was observed around 750-900 μm below the interface between bulk liquid and biofilm. Nitrification activity was observed at around 500-650 μm below the interface. High H_2S production rates was observed around 400-450 μm below the interface, and high H_2S oxidation activity was observed around 550-700 μm below the interface. These results demonstrated that nitrogen removal and sulfate reduction simultaneously occurred inside the MAB. Using O_2, H_2S microsensors, and molecular techniques, Liu et al. (2014) investigated the vertical distribution and activities of sulfate reducing bacteria (SRB) in a piece of MAB. It was observed that oxygen penetrated from the bottom of the gas permeable membrane, and oxygen reached depletion at the interface between bulk liquid and biofilm. H_2S production was observed in the upper 285 μm of biofilm, indicating a high intensity of SRB metabolic activity at the upper section of biofilm. The results of molecular analysis showed that the maximum SRB biomass distributed in upper sections of biofilm, indicating an uneven vertical distribution of SRB inside the MAB.

Babauta et al. (2013) studied the variation of oxygen, hydrogen peroxide, and pH in cathodic biofilms. Pure culture biofilms of *Leptothrix discophora SP-6* and river-water biofilms were compared. The authors reported a correlation between oxygen consumption, hydrogen peroxide accumulation, and cathodic current generation. The authors also reported a reduction of overpotential for oxygen reduction and the generation of a large

cathodic current when polarized cathodes were colonized by cathodic biofilms. The understanding of microscale gradients of chemical species analyzing the chemical gradients with cathodic performance is important for designing cathodes with better performance.

Ning et al. (2014) developed a new approach to determine the thicknesses of the aerobic and anaerobic layers of a biofilm based on the oxygen concentration profiles of the biofilm. The oxygen distribution of a biofilm sampled from a sequencing batch biofilm reactor (SBBR) was measured using microsensors. The maximum and average thicknesses of the tested biofilm was determined to be 640 and 365 μm, respectively. The mean thicknesses of the anaerobic and aerobic layers were determined to be 240 and 270 μm, respectively. The method developed by the authors is a new approach to speculate biofilm structure using the oxygen profiles of biofilm.

Pabst et al. (2016) developed an experimental model to simulate structural and functional characteristics of biofilm infection in mucus or compromised tissue. In these infections, biofilm interspersed in a layer of gel matrix. CLSM studied showed that biofilm distributed throughout the gel matrix in the form discrete aggregates. Oxygen microsensor analysis showed that oxygen concentration decreased with increasing depth in biofilm, reaching 3% of air saturation at depth of 500 μm. An anaerobiosis-responsive fluorescent reporter gene was induced in regions where oxygen concentration was low, confirming biologically-relevant hypoxia. The experimental model developed in this study captured key features of biofilm in mucus or compromised tissue.

Wang et al. (2017) dynamically analyzed the microdistribution, diffusion, and reaction of oxygen in biofilms. Analysis on the oxygen transfer mechanisms in moving biofilms has

been a challenge due to a lack of effective tools. The authors employed a novel experimental device, Oxygen Transfer Modeling Device (OTMD), to accurately simulate the local environment around biofilm in an operating RBC. The variation of oxygen concentration with depth in biofilm and with time were measured using oxygen microsensors. The oxygen transfer in biofilm was also modelled mathematically. The experimental data confirmed well with model prediction, indicating that OTMD device was reliable and mathematical model was well-founded.

Kiamco et al. (2017) studied biofilm on wound surfaces using oxygen and pH microsensors. The repair of tissues requires oxygen, and a low pH condition is advantageous to epithelialization and the release of oxygen from blood. Biofilm on wound surfaces are commonly treated using hyperosmotic agents (e.g. medical-grade honey and cadexomer iodine) in combination with antibiotics (e.g. vancomycin or ciprofloxacin). In the experiment, the biofilm was treated using hyperosmotic agents combined with antibiotics, and then the variation of pH and oxygen concentration within biofilm depth, and the variation of oxygen consumption rates were investigated using microsensors. The authors reported a longer penetration depth of oxygen when the biofilm was challenged by cadexomer iodine combined with vancomycin or ciprofloxacin.

As is seen above, oxygen microsensors are powerful research tools for evaluating important structural and functional characteristics of biofilms. However, all studies cited above investigated biofilms using 1-D oxygen profiles. The limited number of 1-D oxygen profiles might result in a loss of important information about the 3-D distribution of oxygen due to the 3-D heterogeneity of biofilm. To overcome this knowledge gap, de la Rosa and Yu (2005) mapped the 3-D distribution of oxygen in mature wastewater biofilms with a thickness from 630 to 1600 μm. It was reported that the level of the oxygen heterogeneity

decreased with the increasing depth inside biofilms, forming stratification. The decreasing heterogeneity of oxygen from biofilm/bulk liquid interface to the substratum indicated a cell-cluster-like structure at upper sections of biofilm and a compact base layer at deep sections of biofilm. It was also reported that pockets of dissolved oxygen existed in deep sections of biofilm. However, as is discussed in the introduction section, the way of presenting the 3-D oxygen profiles was not effective. Therefore, there is a need to develop a method to better present the 3-D oxygen microelectrode data in order to better understand oxygen penetration and 3-D heterogeneity of wastewater biofilms.

2.2 3-D reconstruction of biofilm structure

The 3-D heterogeneous structure of biofilms are important for the understanding of mass transfer from bulk liquid into biomass, and the understanding of complex microbial activities within biofilm. The application of 3-D optical imaging techniques greatly improved our visualization of the complex structural and functional characteristics within biofilms (Lawrence et al., 1991). 3-D reconstruction from CLSM image stacks is the most important technique for the evaluation of 3-D structure of biofilms. Using appropriate software, sequential 2-D CLSM images acquired at different depths can be stacked to reconstruct biomass distribution in 3-D space. This section presents important contributions about reconstructing 3-D biofilm structure from CLSM image stacks.

Jin et al. (2006) characterized the structure of biofilms deposited on the membrane surface of membrane bioreactors (MBRs) using 3-D CLSM reconstruction. The 3-D structure of biofilm was reconstructed using Imaris software, and the porosity parameters of biofilms were quantified using ISA3D, a Matlab program created by Beyenal et al. (2004) for 3-D CLSM analysis. The porosity parameters of biofilm calculated from CLSM image was validated by comparing calculated values with experimentally measured values.

Bridier et al. (2010) proposed a high throughput method for analyzing structure-function relationships of biofilms based on CLSM reconstruction combined with 96-wells microtiter plates. The 3-D structures of biofilms formed by multiple opportunistic pathogens were reconstructed using Imaris software. Several 3-D structures, such as hollow voids of certain bacteria species, were identified for the first time. The authors also observed specific 3-D structures which were reported in previous studies, such as the mushroom-like structure of specific bacteria species.

Fernández et al. (2016) modelled the effect of fluoridated toothpastes on oral biofilm architecture and enamel demineralization. The 3-D biofilm architecture was reconstructed using Imaris software, and the biofilm structural parameters were quantified using COMSTAT program. It was found that SnF_2 toothpaste reduced the biofilm thickness and biomass volume. Enamel demineralization was significantly reduced by both NaF and SnF_2 toothpaste, while SnF_2 toothpaste is more effective in reducing demineralization.

Harrison et al. (2006) described a detailed procedure for processing of CLSM image stacks using Amira, a commercial virtual reality package, to create 3-D visualizations of biofilm microorganisms. The visualization functions used include isosurface rendering and volume rendering. The authors also combined 3-D visualization techniques with high-throughput susceptibility tests to analyze structures and functions of biofilms under multivariate growth and exposure conditions.

Klug et al. (2016) observed the survival of an oral biofilm and the changes in microbial community within biofilm over time. The biofilm grew inside a patient's mouth before being transferred outside to a biofilm reactor for incubation. The biofilm structure was

observed using CLSM, and Amira software was used to generate 3-D structure from CLSM image stacks. It was found that the *in vitro* survival of native oral biofilm was up to 48 hours, and the complexity of microbial community did not change significantly.

Habimana et al. (2017) investigated the effect of permeate flux on biofilm-induced biofouling development in membrane filtration processes. The biofilm structure and the spatial distribution of live/dead cells were analyzed using CLSM together with live/dead staining technique. The 3-D structure of biofilms were reconstructed using ImageJ software. The authors reported a significant increase of biomass at low-flux condition, indicating that the proliferation of bacteria was impeded at high-flux conditions.

Allen et al. (2018) studied the effect of extrinsic factors on the structural and mechanical properties of biofilms. The extrinsic growth conditions studied included shear condtions, nutrient levels, and cultivation time. CLSM was used to determine biofilm structure, and ImageJ software was used to create 3-D images. Atomic Force Microscopy (AFM) was used to determine mechanical properties of biofilms. It was found that biofilm grew in low nutrient conditions and high shear rates developed better, and these biofilms were more adhesive compared with biofilms grew in high nutrient conditions and low shear rates.

As is seen above, 3-D reconstruction from CLSM image stacks has become an important technique for biofilm research. The software and programs used for 3-D reconstruction include Imaris, Amira, ImageJ, etc. These 3-D reconstruction software allow for reading sequential images to create visualization, while they do not provide function for directly reading and visualizing 3-D microsensor data which is in the form of multi-dimensional matrix. To my best knowledge, there is no available software for visualizing the 3-D oxygen profiles determined by microsensor. Therefore, there is a pressing need to develop

a software or program for effective visualization of 3-D oxygen profiles in order to better understand the structural and functional characteristics of biofilms.

3 Method study and development

3.1 A review of the method for measuring 3-D oxygen profiles

The 3-D data visualized in this study was the data measured by de la Rosa and Yu (2005) rather than measured by myself. To show the distribution of oxygen in three dimensions, the authors in the previous study aligned many 1-D oxygen concentration profiles which are perpendicular to the substratum, forming 3-D oxygen profiles. For each 1-D oxygen concentration profile that is perpendicular to substratum, the distance between adjacent data point is 80 μm. The calibration curve of oxygen microsensor was constructed based on three data points (as shown in Fig 3-1). The R^2 of linear regression was 1, indicating a clear linear relationship between current signal and oxygen concentration. The high value of R^2 of calibration curve showed that the oxygen microsensor satisfy the requirements for measuring oxygen profile.

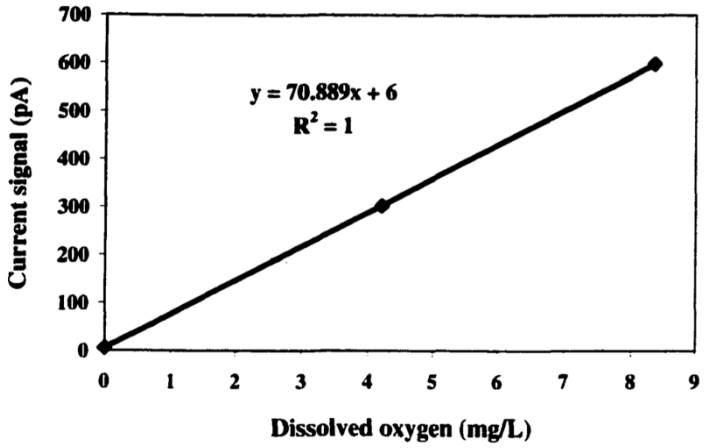

Fig 3-1 Calibration curve of oxygen microsensor for 3-D oxygen profiles

(Lu & Yu, 2002)

The biofilm surface was determined visually by using the microsensor and microscope. A horizontal artificial plane which was above the biofilm sample was used as a reference plane. At every location where each 1-D oxygen profile was measured, the tip of microsensor was moved down from the artificial plane to the position exactly on the biofilm surface, and the interval between artificial plane and biofilm surface at every location was recorded. The maximum resolution for the vertical movements of oxygen microsensor was 0.1 μm.

In the previous study, two strategies were used for aligning 1-D profiles to form 3-D oxygen profiles. The first strategy used a horizontal artificial plane as a physical reference. In this strategy, all the first measurements of each 1-D profiles were aligned in the horizontal artificial plane. The other measurements were aligned in subsequent horizontal planes which are parallel to the artificial plane at different depths. This means that each 3-D oxygen profile acquired using the first strategy is a stack of 2-D layers of data at different depths. Each layer of data is measured on subsequent horizontal planes parallel to the artificial plane instead of biofilm surface.

The second strategy used the heterogeneous biofilm surface as a physical reference. In this strategy, all the first measurements of each 1-D profiles were aligned on the biofilm surface, oxygen concentrations were then determined at exact positions above and below the biofilm surface. This means that each 3-D oxygen profiles acquired using the second strategy is also a stack of 2-D layers of data at different depths. This time, each layer of data is measured on subsequent curved surfaces which are parallel to the heterogeneous biofilm surface instead of the artificial plane. To my best knowledge, there is no available software that support directly reading multi-dimensional matrix with curved layers of data, while there is commercially available software allows for direct reading and processing

multi-dimensional matrix with horizontal layers of data. Consequently, the 3-D oxygen profile acquired using the first strategy was visualized only in this study.

Fig 3-2 (a) is the coordinate system used in this study, and Fig 3-2 (b) is a schematic diagram of horizontal layers acquired from 3-D oxygen measurements. As shown in Fig 3-2 (b), the distances between adjacent individual oxygen profiles in the x and y direction are defined as dx and dy respectively, and the distance between adjacent layers is defined as dz. The values of dx, dy, and dz in the previous study are 100 μm, 100 μm and 80 μm respectively. The number of individual oxygen profiles per layer is 100 in a 10×10 array.

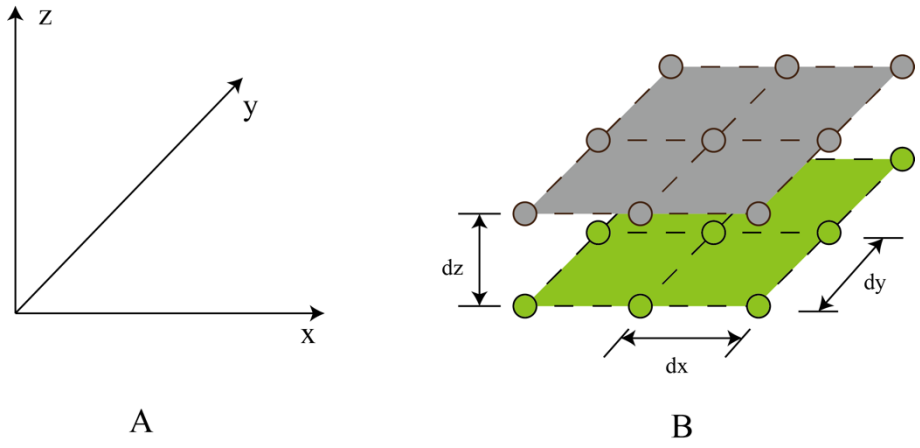

Fig 3-2 Overview of coordinate system and horizontal data layers

(A) Coordinate system used in this study (B) Definition of dx, dy, dz in relationship to horizontal layers and data points in 3-D oxygen measurement. Each individual circle represents a data point in 3-D oxygen measurement

3.2 Selection of software

As is discussed in Section 3.1, the 3-D oxygen profiles of biofilm are in the form of multi-dimensional matrix. It is necessary to choose a correct software for effective visualization of the multi-dimensional matrix. A possible option is to use the currently available software

which allows for 3-D reconstruction of biofilm structure (e.g. Imaris, Amira, and ImageJ). After a careful reading of the manuals of these software, it was found that only data in the form of sequential images were supported, while data in the form of multi-dimensional matrix were not supported. Therefore, an image sequence must be firstly created based on the multi-dimensional matrix so that the data can be imported. An individual image can be created based on one horizontal layer of data in the multi-dimensional matrix. Due to the large distance between adjacent horizontal layers (dz= 80 μm), several images need to be interpolated between adjacent horizontal layers in order to create an image sequence with sufficient density. Overall, it takes a lot of effort to create an image sequence for data importing if the current available 3-D reconstruction software is used in this study.

Another option is to visualize the 3-D oxygen profiles using software that allows for directly importing and processing multi-dimensional matrix data. Matlab is a powerful software that allows for multi-dimensional matrix manipulation, plotting, and visualization (Nakamura, 2002). Matlab allows for reading multi-dimensional matrix directly, which means that the effort for creating an image sequence can be omitted when using Matlab. More importantly, the visualization functions provided by Matlab completely cover all the visualization functions provided by software for 3-D biofilm reconstruction (Mathwork, 2018f). Overall, the use of Matlab does not require complicated preparation steps, while the same visualization effects can be realized compared with using 3-D biofilm reconstruction software. Therefore, Matlab was selected for 3-D visualization of oxygen distribution within biofilm in this study.

Multi-dimensional matrices are more commonly referred to as volume data by Matlab users. Matlab supports the visualization of volume data by creating graphical representations of these data sets that are defined on 3-D grids. The steps of visualizing volume data were

summed up Mathworks (2018f). Basically four steps are needed for composing the final scene of visualization:

- Step 1: Determine the range of data values. A knowledge of the range of data is necessary for Matlab users to determine the range of the coordinate system.
- Step 2: Select appropriate visualization functions. The visualization functions are usually selected based on the purposes of visualization.
- Step 3: Define the perspective. The perspective parameters include camera position, aspect ratio, scaling factors, project types, and so on. The information conveyed by a 3-D visualization will be greatly enhanced when perspective parameters are carefully composed and adjusted.
- Step 4: Specify colors and add lighting. In the visualization of volume data, colors are used to covey data values. Appropriate lighting is sometimes helpful in creating a three-dimensional perspective and is helpful in enhancing the visibility of surface shape.

The visualization of 3-D oxygen profile through steps 1-4 will be discussed in the following sections. Step 1 will be discussed in Section 3.3; Step 2 will be discussed in Section 3.5, 3.6, and 3.7; Step 3 will be discussed in Section 3.8; Step 4 will be discussed in Section 3.9.

3.3 Selection of data layers for visualization

A total of 11 horizontal data layers were piled up for visualization. Since the visualization of 3-D oxygen heterogeneity inside biofilm was the primary focus of this study, the top layer (layer 11, as shown in Fig 3-3) in this study was a horizontal data layer that was closest to the zenith of biofilm. The maximum thickness of Sample 1 in the previous study

is 834 μm, and the top layer chosen in this study is 820 μm above the substratum. The bottom layer (layer 1, as shown in Fig 3-3) in this study was a horizontal data layer that was deepest in the previous study, which is 20 μm above the substratum. The distance between the top layer and bottom layer is 800 μm. The dimension of visualization volume in this study is 900 μm ×900 μm ×800 μm, and there are 1100 individual data points in the visualization volume in a 10×10×11 array. Correspondingly, the range of x, y, and z axes were set as 0 to 900 μm, 0 to 900 μm and 20 to 820 μm respectively (as shown in line 30 of Appendix A). For the convenience of data import, all 11 layers of data were copied into 11 individual worksheets in the same .xls file named 'Sample1.xls'. The 11 worksheets were named as 'layer1', 'layer2', ...'layer11' in 'Sample1. xls'. The biofilm thickness data (which is also in a 10×10 array) was copied into another individual worksheet in 'Sample1. xls'.

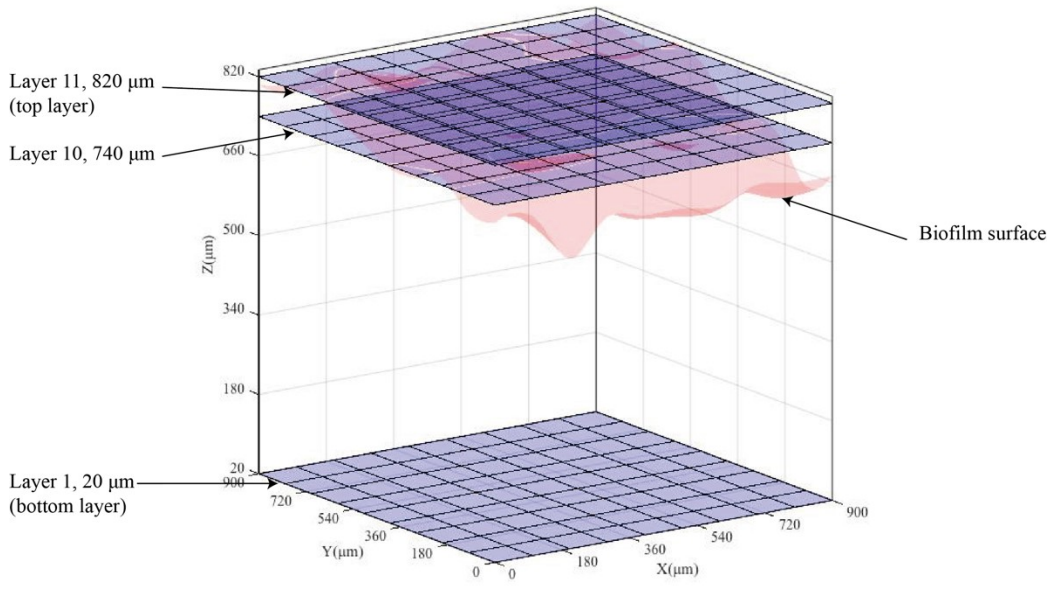

Fig 3-3 Schematic of 11 layers of data in the visualization volume

3.4 Data import and interpolation

A 10×10×10 3-D mesh was created to contain 3-D oxygen data (as shown in line 3 of Appendix A). The 3-D oxygen data was imported using function **`xlsread`** (as shown in line 5-15 of Appendix A). A 10×10 2-D mesh was created to contain 2-D biofilm surface data (as shown in line 22 of Appendix F). The 2-D biofilm surface data was also imported using function **`xlsread`** (as shown line 23 of Appendix F).

The data density of both 3-D oxygen data and 2-D biofilm surface data is low. If curved surfaces (e.g. biofilm surface, isosurface) were directly created using visualization functions, the surfaces will appear to be discontinuous due to the low data density. Thus, interpolation is needed for smoothing data in order to create better visualization scenes. Matlab provides three basic interpolation methods: **`nearest`**, **`linear`**, and **`cubic`** (as shown in Table 3-1). The schematic diagram of three interpolation methods is shown in Fig 3-4. The **`nearest`** method was not used in this study because it is a discontinuous interpolation method. The interpolated value obtained using the **`nearest`** method was a copy of value at the nearest grid point, which would create discontinuous interpolated surfaces. Compared with the **`linear`** method, the **`cubic`** method is more effective in creating smooth and continuous interpolated data, while **`cubic`** interpolation might cause distortion of data that we cannot assess due to increased continuity and smoothness after interpolation. Since the change of oxygen concentration from amongst data points in 3-D oxygen profile is unclear, it is possible that linear method allows for presenting the oxygen concentrations in biofilm close to its actual concentrations. Consequently, the **`linear`** method was used for the interpolation of 3-D oxygen data and 2-D biofilm surface data. The effects of different interpolation methods on creating curved surfaces were also discussed in Section 4.1.3.

Table 3-1 Interpolation methods provided by Matlab

(Reprinted from Mathwork, 2018c)

Method	Description	Continuity	Comments
`nearest`	The interpolated value at a query point is the value at the nearest sample grid point.	Discontinuous	Requires two grid points in each dimension; Fastest computation with modest memory requirements.
`linear`	The interpolated value at a query point is based on linear interpolation of the values at neighboring grid points in each respective dimension. This is the default interpolation method.	C^0 *	Requires at least two grid points in each dimension; Requires more memory than '`nearest`'.
`cubic`	The interpolated value at a query point is based on a cubic interpolation of the values at neighboring grid points in each respective dimension. The interpolation is based on a cubic convolution.	C^1 **	Grid must have uniform spacing in each dimension, but the spacing does not have to be the same for all dimensions; Requires at least four points in each dimension; Requires more memory and computation time than '`linear`'.

* C^0 continuity: curves are continuous while first derivatives are not necessarily continuous

** C^1 continuity: curves are continuous and first derivatives are continuous

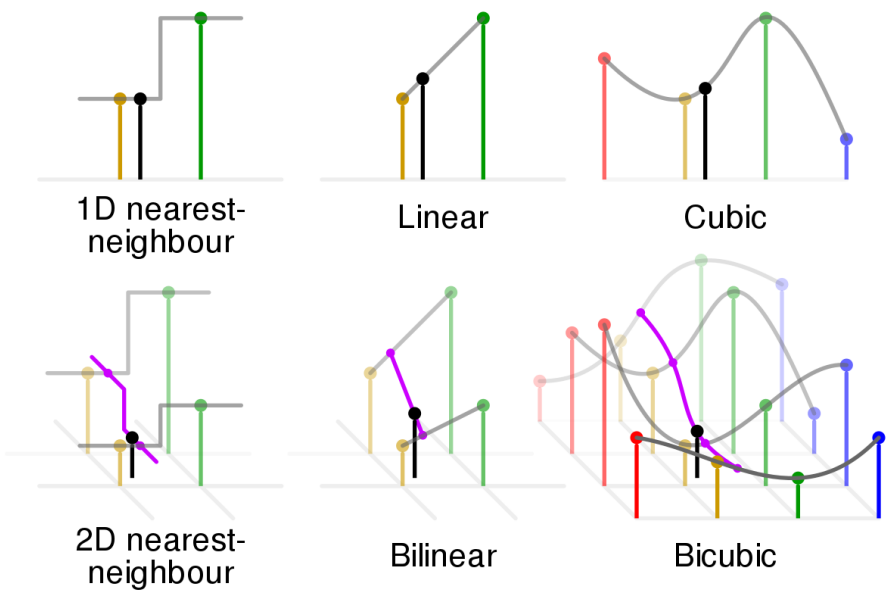

Fig 3-4 Schematic diagram of 'nearest', 'linear', and 'cubic' interpolation

The black point represents interpolated data. The yellow, green, red and blue points represent neighbouring data. ("Bicubic interpolation", (n.d.))

A denser 3-D mesh was created to contain interpolation for oxygen concentration (as shown in line 17 of Appendix A). A denser 2-D mesh was created to contain interpolation for biofilm surface data (as shown line 25 of Appendix F). 3-D interpolation was performed using function **`interp3`** (as shown in line 19 of Appendix A), and 2-D interpolation was performed using function **`interp2`** (as shown in line 26 of Appendix F).

3.5 Creation of the biofilm surface, slices and isosurfaces

The biofilm surface was created using the function **`surf`** (as shown in line 36-38 of Appendix B). The transparency and edge color of the biofilm surface can be adjusted by changing arguments in line 37 and 38 of Appendix B.

Colormap slices were created using the function **`slice`** (as shown in line 24 of Appendix A). The position and orientation of colormap slices can be adjusted by changing arguments in line 21-23 of Appendix A. A colormap slice allows for the converting values of multi-dimensional matrix to colors, which are useful for probing into matrix to seek interesting regions. Fig 3-5 is a sample of colormap slices adapted from Matlab documentation.

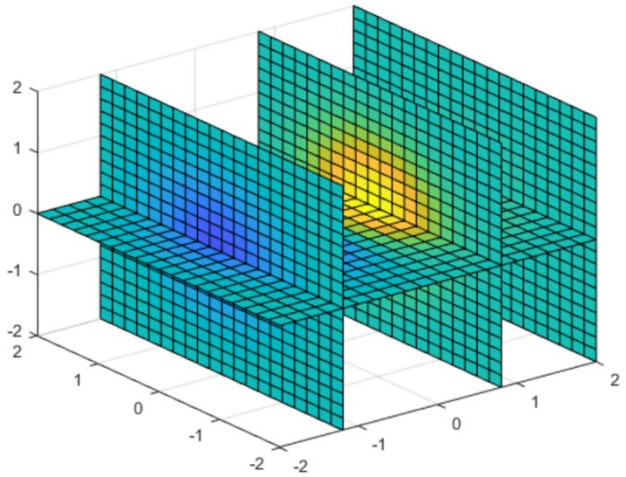

Fig 3-5 Sample colormap slices in Matlab documentation

(Reprinted from Mathwork, 2018c)

Contour slices were created using the function **`contourslice`** (as shown in line 24 of Appendix B). The position and orientation of contour slices can be adjusted by changing arguments in line 21-23 of Appendix B. The number of contours on each slice can be adjusted by changing the last argument of line 24 of Appendix B. A contour slice connects data with the same value on the plane of interest using contours. Fig 3-6 is a sample of contour slices adapted from Matlab documentation.

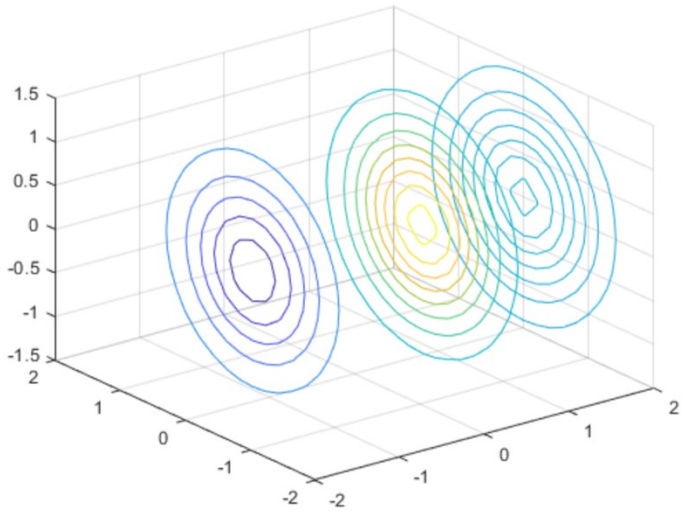

Fig 3-6 Sample contour slices in Matlab documentation

(Reprinted from Mathwork, 2018d)

Isosurfaces were created using the function **`patch`** and **`isonormals`** (as shown line 21-22 of Appendix C). The face color, edge color and transparency of isosurfaces can be adjusted by changing arguments in line 23-24 of Appendix C. An isosurface connects data with the same value within the whole multi-dimensional matrix. Fig 3-7 is a sample of isosurface slices adapted from Matlab documentation.

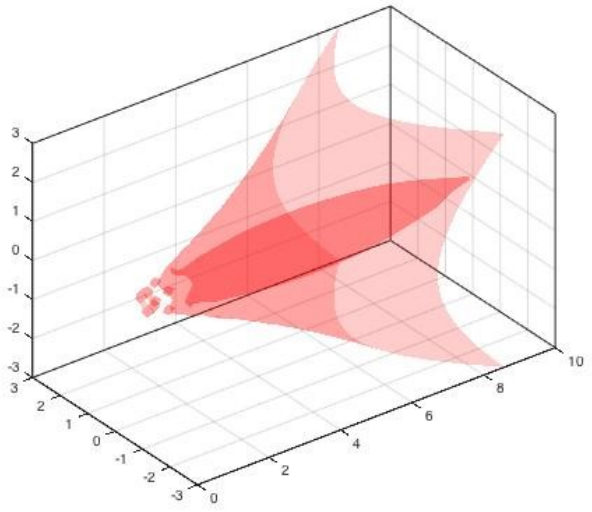

Fig 3-7 A sample isosurface in Matlab documentation

(Adapted from Mathwork, 2018e)

3.6 Creation of curved colormap slices

In order to visualize the oxygen distribution on the biofilm surface, a curved colormap slice was created using function using the function **`slice`** (as shown line 28 of Appendix F)**.** By changing the last three arguments of slice function to a group of variables that define a curved surface, data in the multi-dimensional matrix will be showed along the nonplanar slice. Fig 3-8 is a sample of curved colormap slices reprinted from Matlab documentation.

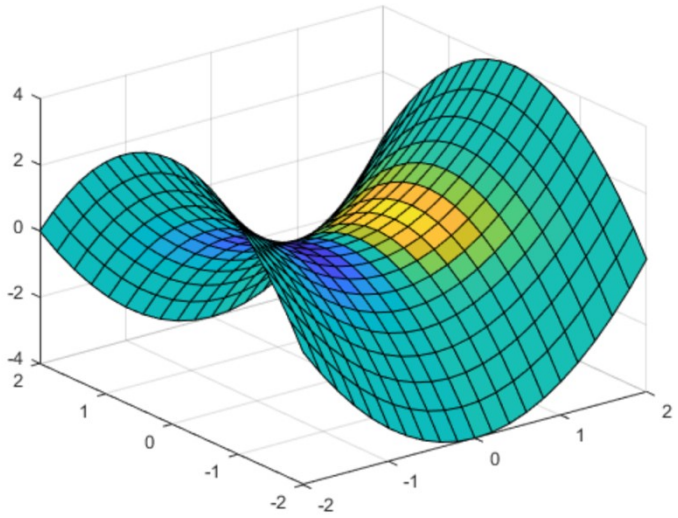

Fig 3-8 A sample curved colormap slice in Matlab documentation

(Reprinted from Mathwork, 2018c)

3.7 Visualizing matrices with different dimensions in the same scene

In order to visualize the oxygen distribution near the biofilm surface, the data of biofilm surface and 3-D oxygen need to be plotted in the same visualization scene. The biofilm surface data is in the form of 3-D matrix (x, y coordinates and thickness), while the spatial

oxygen data is in the form of 4-D matrix (x, y, z coordinates and oxygen concentration). Due to different dimensions of the two types of data, if 3-D oxygen data are directly plotted in the same scene after the plotting of biofilm surface data, the existing plot of biofilm surface will be deleted. Therefore, a question arises on how to simultaneously visualize matrices with different dimensions in the same scene.

According to Matlab documentation, the **`hold on`** command can retain plots in the current visualization scene so that new plots added to the scene do not delete the existing plots (Mathwork, 2018b). Consequently, the **`hold on`** command was used to retain the 3-D oxygen distribution in the same visualization scene containing the biofilm surface (as shown in line 31 of Appendix G). By using the **`hold on`** command, 3-D oxygen distribution at the biofilm surface can then be effectively visualized.

3.8 Creation of animations

Using slices and surfaces from specific positions, the visualization functions in Section 3.5, 3.6, and 3.7 can create effective visualization of 3-D oxygen distribution in wastewater biofilms from specific perspectives. However, all these types of visualization are static. A more comprehensive visualization can be created using animation, which can show the 3-D distribution of oxygen from dynamic perspectives and using slices with changing positions. Therefore, several animations were created for better visualization of the 3-D oxygen distribution in wastewater biofilms.

An animated version of colormap slice (an animated Fig 4-1 (C)) was created for the 3-D visualization of oxygen distribution. To create the animated Fig 4-1 (C), a loop variable **`i`** was included into the arguments of the function **`slice`** for the production of moving colormap slices (as shown in line 22 and 23 of Appendix D), and the loop variable **`i`** was

included into the function **`view`** for the production of a rotating perspective (as shown in line 45 of Appendix D). A matrix **`M`** was created for saving the animation (as shown in line 21 of Appendix D), and the function **`getframe`** (as shown in line 46 of Appendix D) was used to deliver the animation into matrix **`M`**. The function **`movie2avi`** was used to save the animation into a .avi file (as shown in line 49 of Appendix D). The frame rate of the animated Fig 4-1 (C) is 30 fps and the animation lasts 20 seconds.

An animated version of isosurfaces (an animated version of Fig 4-3 (A)), an animated version of oxygen distribution on biofilm surface (an animated version of Fig 4-5), and animated version of oxygen distribution near biofilm surface (an animated version of Fig 4-6) were also created. The key steps for creating other animations were same as those for creating the animated version of Fig 4-1 (C). A loop variable **`i`** was included into the arguments of function **`view`** for the production of rotating perspectives, and the loop variable **`i`** was included into the arguments of function **`slice`** for the production of moving slices. A matrix **`M`** was created for saving the animation, and the function **`getframe`** was used to deliver the animation into matrix **`M`**. The function **`movie2avi`** was used to save the animation into a .avi file.

3.9 Addition of lighting

Appropriate lighting can be used to enhance the surface shape and to create a 3-D perspective of the visualization scene (Mathworks, 2018f). Fig 3-9 is a sample for the effect of light in enhancing the visibility of surface shape. It can be observed from Fig 3-9 that the shape of sample isosurface becomes more noticeable after the addition of lighting.

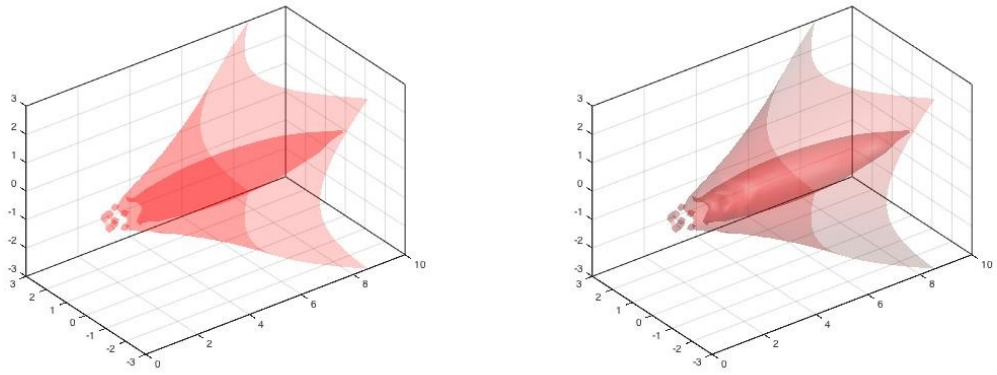

(A) (B)

Fig 3-9 Effect of lighting in enhancing the visibility of surface shape

(A) In the absence of lighting (B) In the presence of lighting (Adapted from Mathwork, 2018e)

It is necessary to add appropriate lighting in order to enhance the visibility of the curved surfaces that were created in this study. Matlab provides two lighting methods: **`lighting flat`** and **`lighting gouraud`** (Mathworks, 2018g). **`Lighting flat`** produces uniform lighting across each of the faces of the object, which is recommended for the visualization of faceted objects. **`Lighting gouraud`** calculates the vertex normals and interpolates across the faces, which is recommended for the visualization of curved surfaces. Since the purpose of adding lighting in this study is to make the surfaces more noticeable, **`lighting gouraud`** was used in this study (as shown in line 46 of Appendix C). Lighting was not used in the visualization of oxygen distribution on biofilm surface, because the lighting will interfere with the colors on the biofilm surface, which makes it hard to distinguish colors and oxygen conentrations on the biofilm surface.

3.10 System requirements

Only the basic module of the Matlab commercial package is required for the running of Matlab programs developed in this study. An ordinary desktop or laptop computer with 4 GB free RAM memory is sufficient for the running of Matlab programs. The programs were tested using Matlab R2014b under Mac OS X EI Capitan, version 10.11.3.

4 Results and discussion

4.1 3-D visualization of oxygen distribution in wastewater biofilm

The first question of interest in this study is how to present the oxygen distribution in biofilms using 3-D visualization instead of using individual 2-D cross sections. To overcome this knowledge gap, colormap slices, contour slices, isosurfaces, and animations were created for the 3-D visualization of oxygen distribution.

4.1.1 Colormap slices

By copying and pasting the program in Appendix A to the Matlab command line and running the program, Fig 4-1 (A) can be produced. By changing the arguments in line 21-23 of Appendix A and then running the program, Fig 4-1 (B) and (C) can be produced. Fig 4-1 (A) shows the oxygen distribution within biofilm on individual horizontal slices that are 100 μm, 260 μm, 420 μm, 580 μm, and 740 μm above the substratum respectively. Fig 4-1 (A) also allows for the comparison of oxygen heterogeneity on horizontal slices at different depths. It is apparent that oxygen heterogeneity descends from the surface sections of biofilm to the deep sections of biofilm. Fig 4-1 (B) shows biofilm oxygen distribution on individual slices that are perpendicular to x axis at 100 μm, 260 μm, 420 μm, 580 μm, and 740 μm respectively. Fig 4-1 (B) also allows for the comparison of oxygen heterogeneity on vertical slices at different positions. Fig 4-1 (C) allows for the simultaneous visualization and analysis of oxygen distribution on slices that are perpendicular to x, y, z axes respectively. In sum, the visualization of biofilm oxygen distribution via 3-D colormap slices provides improved 3-D visualization compared to conventional visualization of oxygen distribution where individual slices of oxygen concentration are presented in individual 2-D figures.

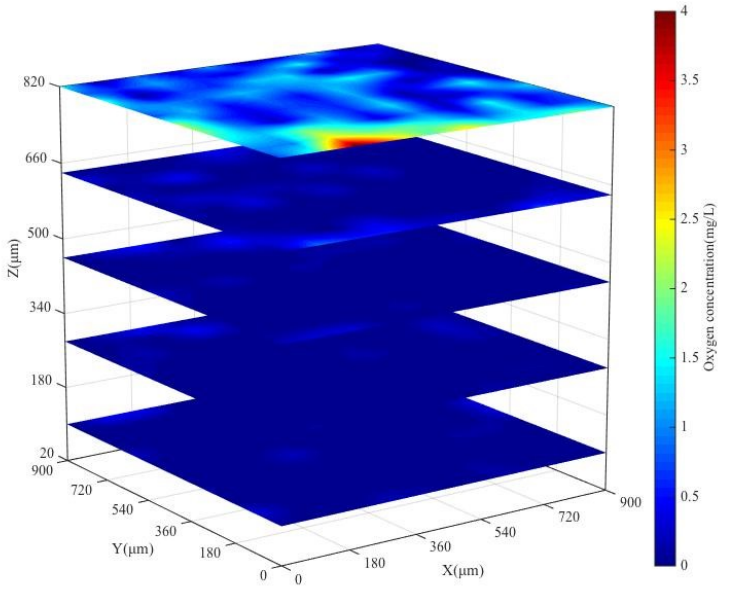
Z(μm)
820
660
500
340
180
20
Y(μm)
900
720
540
360
180
0
X(μm)
0
180
360
540
720
900
Oxygen concentration(mg/L)
4
3.5
3
2.5
2
1.5
1
0.5
0

(A)

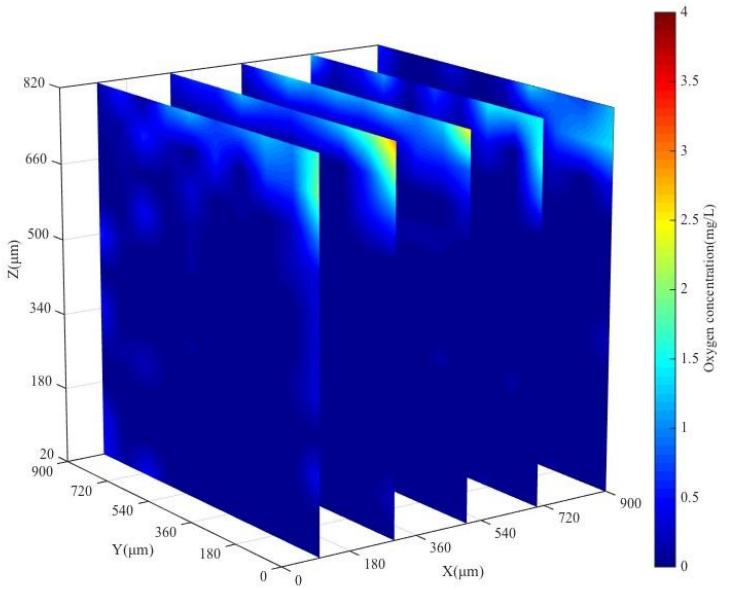
Z(μm)
820
660
500
340
180
20
Y(μm)
900
720
540
360
180
0
X(μm)
0
180
360
540
720
900
Oxygen concentration(mg/L)
4
3.5
3
2.5
2
1.5
1
0.5
0

(B)

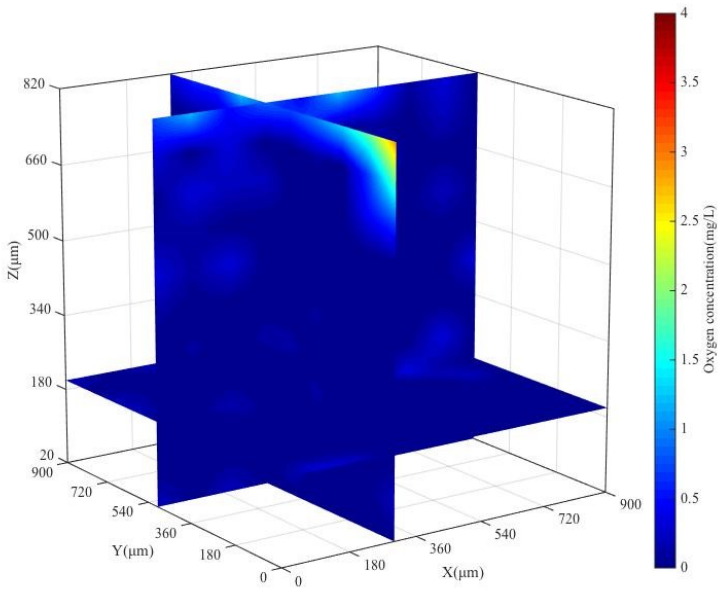

(C)

Fig 4-1 3-D distribution of oxygen in biofilm visualized by colormap slices (A) Horizontal colormap slices that are perpendicular to z axis at 100 μm, 280 μm, 460 μm, 640 μm, and 820 μm respectively (B): Vertical colormap slices that are perpendicular to x axis at 100 μm, 300 μm, 500 μm, 700 μm, and 900 μm respectively (C) Colormap slices that are perpendicular to x, y, and z axes at 300 μm, 500 μm, and 200 μm respectively

4.1.2 Contour slices

By copying and pasting the program in Appendix C to the Matlab command line and running the program, Fig 4-2 (A) can be produced. By changing the arguments in line 21-23 of Appendix C and then running the program, Fig 4-2 (B) can be produced. Fig 4-2 (A) visualizes 3-D biofilm oxygen distribution by presenting oxygen contours on horizontal slices that are 400 μm, 640 μm above the substratum respectively. Fig 4-2 (A) also allows for the comparison of oxygen contour on horizontal slices at different depths. Fig 4-2 (B)

allows for the simultaneous visualization and analysis of oxygen distribution on contour slices that are perpendicular to x, y, and z axes respectively. In sum, 3-D visualization of biofilm oxygen distribution via 3-D contour slices provides another unique perspective for presenting 3-D details of biofilm spatial oxygen heterogeneity.

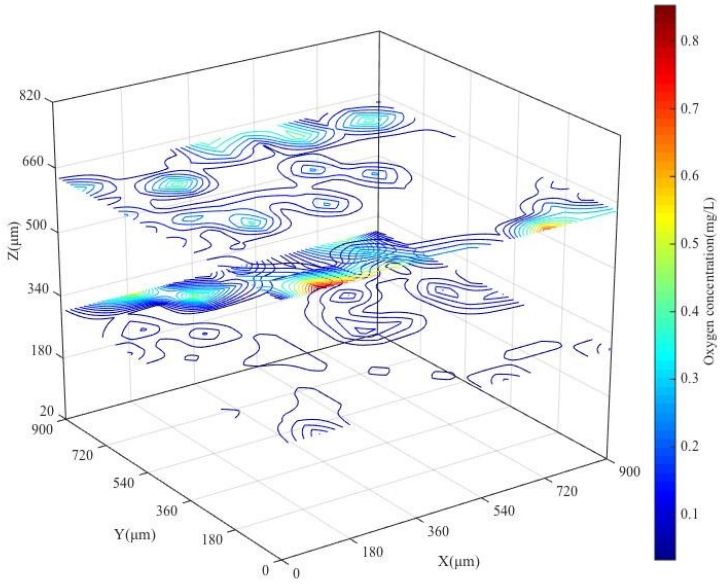

(A)

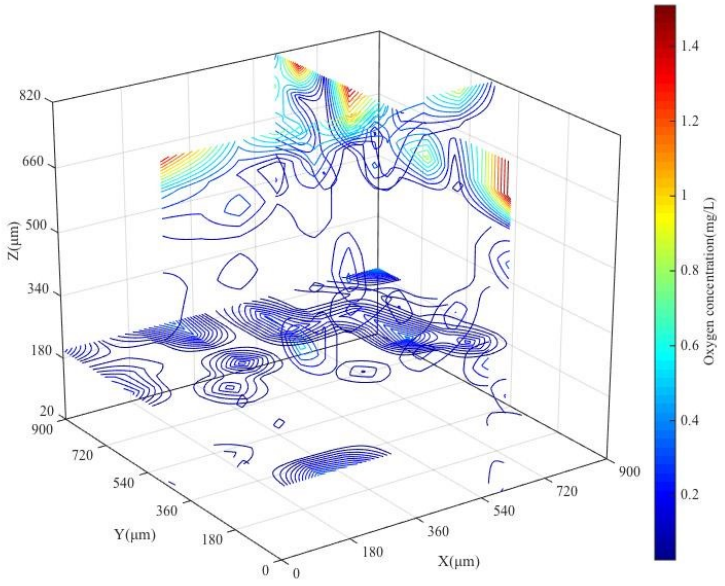

(B)

Fig 4-2 3-D distribution of oxygen in biofilm visualized by contour slices.

(A): Horizontal contour slices that are perpendicular to z axis 300 μm and 640 μm respectively (B): Vertical contour slices that are perpendicular to x, y, and z axes at 600 μm, 450 μm, and 200 μm respectively

4.1.3 Isosurfaces

By copying and pasting the program in Appendix D to the Matlab command line and running the program, Fig 4-3 (A) can be produced. By changing the arguments in line 20, 22, 25, and 27 of Appendix C and then running the program, Fig 4-3 (B) can be produced. The purple surface in Fig 4-3 (A) connects all concentration points of 0.2 mg/L oxygen in the biofilm sample. The green surface in Fig 4-3 (A) connects all concentration points of 0.3 mg/L oxygen in the biofilm sample. The yellow surface in Fig 4-3 (B) connects all concentration points of 0.4 mg/L oxygen in the biofilm sample. The orange surface in Fig 4-3 (B) connects all concentration points of 0.5 mg/L oxygen in the biofilm sample.

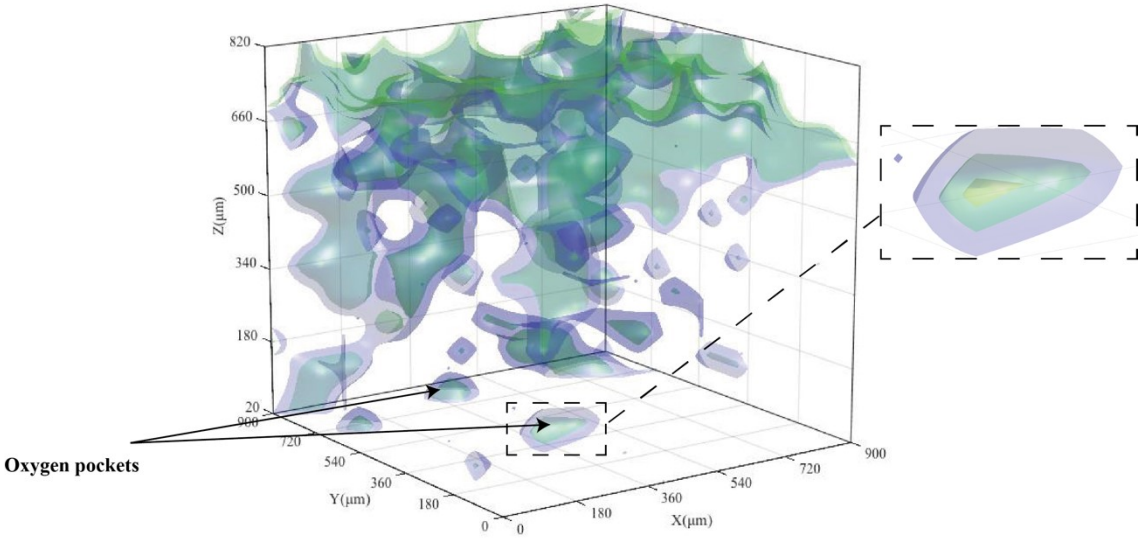

(A)

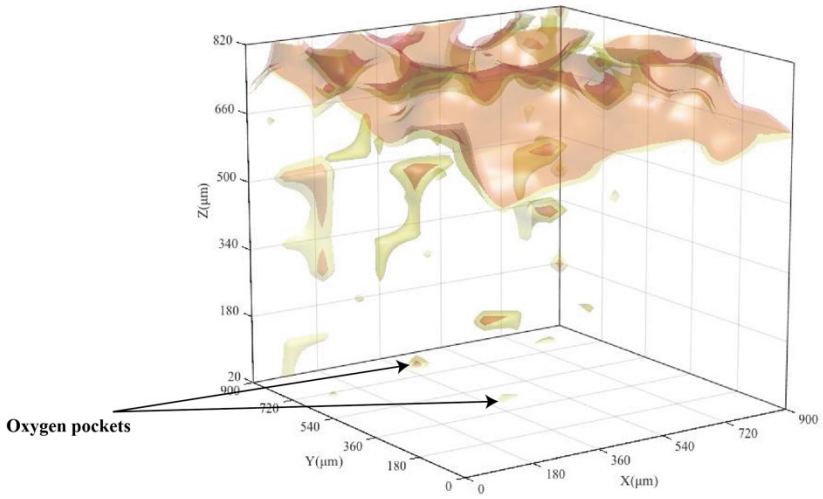

(B)

Fig 4-3 3-D distribution of oxygen in biofilm visualized by isosurfaces

(A) 0.2 mg/L oxygen isosurface (purple) and 0.3 mg/L oxygen isosurface (green). The yellow bubble in the center of big dashed frame represents 0.4 mg/L oxygen isosurface. (B): 0.4 mg/L oxygen isosurface (yellow) and 0.5 mg/L oxygen isosurface (orange).

From Fig 4-3, it can be observed that the oxygen pockets in deep sections of biofilm exist in isolation, which means that the oxygen pockets in deep sections are not connected with the oxygen zone in upper sections of biofilm. The independence of oxygen pockets was not observed in the visualization results of the previous study.

The formation of isolated oxygen pockets might be due to the heterogeneity of metabolic activity in biofilm. The distribution of chemical species in biofilm is simultaneously determined by the diffusion, production and consumption of chemical species (Stewart & Franklin, 2008). The formation of oxygen might be a timely event. During the early stage of biofilm development, the biofilm was thin and oxygen existed within biofilm. As the biofilm developed and its thickness increased, oxygen in some locales of biofilm was not completely consumed. Consequently, oxygen in few locations remained, forming localized microaerobic environment, while the deep section of mature biofilm was largely anoxic. Overall, the independence of oxygen pockets might indicate that biofilm is physiologically heterogeneous, which is consistent with findings from previous studies (Nguyen & Singh, 2006; Stewart & Franklin, 2008).

In addition, the isosurfaces in Fig 4-3 (A) and (B) reveals the 3-D structure of oxygen pockets is ellipsoid (as shown in the dashed frame in Fig 4-3 (A)). The distribution relationship amongst multiple oxygen pockets can also be observed in Fig 4-3 (A) and (B). The structure and distribution relationship of oxygen pockets could not be observed from the visualization results of the previous study. In sum, the 3-D visualization of biofilm

oxygen distribution with isosurfaces is a different visualization approach compared with the visualization of oxygen distribution with colormap slices or with contour slices, and the 3-D oxygen isosurfaces convey crucial information regarding 3-D oxygen heterogeneity in biofilm.

The effects of different interpolation methods in creating isosurfaces are shown in Fig 4-4. Fig 4-4 (A) shows isosurfaces created by using nearest interpolation method. It can be observed from Fig 4-4 (A) that the isosurfaces created by using nearest method are rectangular, which differs greatly from actual situation. Fig 4-4 (B) shows isosurfaces created by using cubic interpolation method. It can be observed from Fig 4-4 (B) that the isosurfaces created by using cubic method are smoother compared with isosurfaces created by using linear method, while the increased smoothness and continuity after cubic interpolation might result in distortion of data that we cannot assess. Consequently, linear method was used in this study to increase the density of raw data.

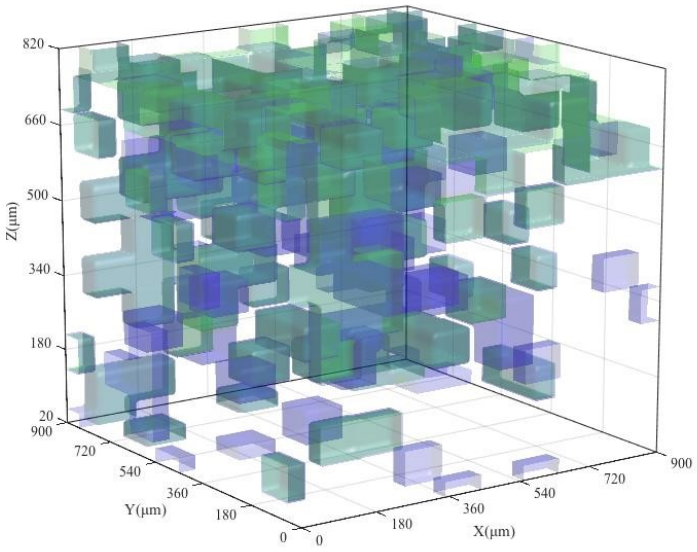

(A)

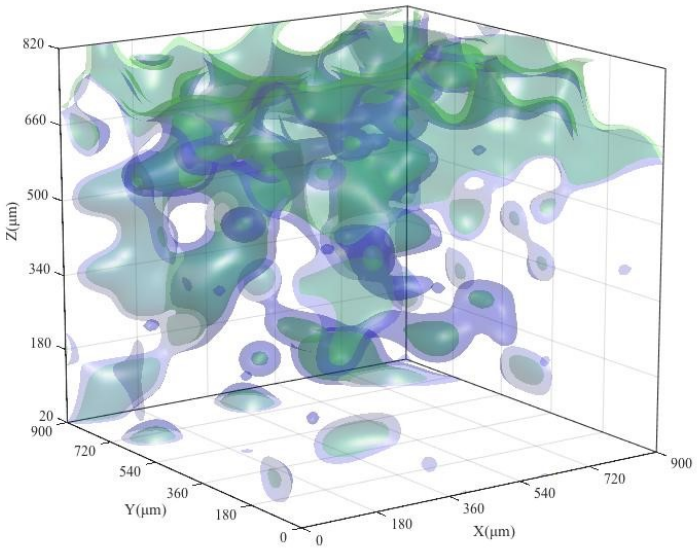

(B)

Fig 4-4 Oxygen isosurfaces created using 'nearest' and 'cubic' interpolation methods. (A) Isosurfaces created by using 'nearest' interpolation method (B) Isosurfaces created by using 'cubic' interpolation method

4.1.4 Animation

By copying, pasting and running the programs in Appendix D and E at Matlab respectively, the animated version of colormap slices (animated Fig 4-1 (C)) and the animated version of isosurfaces (animated Fig 4-3 (A)) can be produced respectively. The animations will be saved as .avi files into Matlab folders. The two animations are also available at YouTube:

Animated version of colormap slices: https://youtu.be/21jR9-nhZ8Y

Animated version of isosurfaces: https://youtu.be/mDAaj7WciyE

These animations with moving colormap slices and with rotating perspective allows for the presentation of more details regarding 3-D oxygen heterogeneity inside biofilm compared with the visualization with static figures.

4.2 3-D visualization of oxygen distribution on and near biofilm surface

The second question of interest in this study is how to visualize the 3-D oxygen distribution on and near biofilm surface. To visualize the oxygen distribution on the biofilm surface, a curved colormap slice which converts the oxygen concentrations to colors was plotted. To visualize the oxygen distribution near biofilm surface, the biofilm surface data and the 3-D oxygen profile were plotted in the same visualization scene. The animated version of the both visualization scenes were also created to present more details about the oxygen distribution on and near biofilm surface.

4.2.1 Oxygen distribution on the biofilm surface

By copying and pasting the program in Appendix F to the Matlab command line and running the program, Fig 4-5 can be produced. Fig 4-5 presents the oxygen distribution on the biofilm surface. The crests and troughs of the surface represent the morphology of biofilm surface, while the different colors on the surface represent different oxygen concentrations. Compared with the previous visualization method that presented the morphology of biofilm surface and the oxygen distribution on biofilm surface by using different figures, Fig 4-5 succeeded in simultaneously visualizing the morphology of biofilm surface in relationship to oxygen distribution on biofilm surface for the first time.

From the colors on the curved surface in Fig 4-5, it can be observed that the oxygen concentrations on the biofilm surface were in the range of 0 to 1.6 mg/L. The oxygen

concentrations in the bulk liquid, which was approximately 800 μm above the biofilm surface, were reported to be higher than 6 mg/L (de la Rosa & Yu, 2005). In the previous study, the decrease of the oxygen concentrations from the bulk liquid to the biofilm surface was explained due to the oxygen-consuming metabolic activity of microorganisms. It can also be observed from Fig 4-5 that the oxygen distribution on the biofilm surface is highly heterogeneous, with oxygen concentrations at some locations reaching up to 1.6 mg/L while at some locations reaching depletion. Fig 4-5 also succeeded in visualizing the heterogeneity of metabolic activity in relation to the morphology of biofilm surface for the first time.

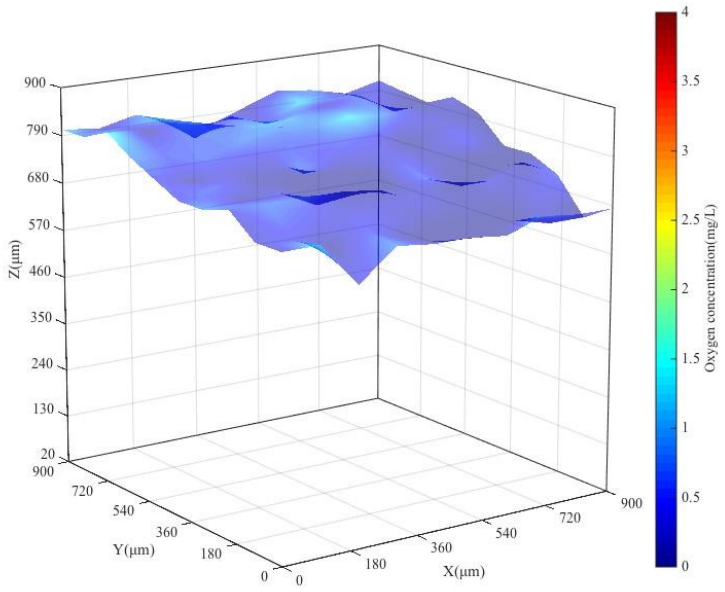

Fig 4-5 3-D visualization of oxygen distribution on biofilm surface

4.2.2 Oxygen distribution near the biofilm surface

By copying and pasting the program in Appendix G to the Matlab command line and running the program, Fig 4-6 can be produced. Fig 4-6 presents both the biofilm surface

and oxygen distribution of the horizontal slice that is 740 μm above the substratum. The biofilm surface is depicted as the brown surface with crests and troughs, while the oxygen distribution at 740 μm horizontal slice is depicted as the plane with different colors corresponding to different oxygen concentration. By superimposing the biofilm surface and oxygen distribution, the curvy line indicating the interception between biofilm surface and horizontal slice can be clearly visualized for the first time. The ratio between water and biomass on a specific horizontal slice can then be calculated based on the interception line. The water/ biomass ratio on a horizontal slice at biofilm surface area is important for comparing the vertical distribution of bacteria biovolume along the biofilm depth, which is useful in understanding structural and functional characteristics of biofilm.

The range of biofilm thickness in this study is 604 to 834 μm. From Fig 4-6, it can be seen that the oxygen concentration at the 740 μm slice is higher where the biofilm is thinner, and the oxygen concentration at the slice is lower where the biofilm is thicker. This phenomenon can be explained by the fact that the oxygen concentration detected at places with thinner biofilm is the oxygen concentration of concentration boundary layer, whereas the oxygen concentration detected at places with thicker biofilm is the oxygen concentration of the internal biomass. Due to the metabolism of biomass, the internal oxygen concentration of the biomass is slightly lower compared with the oxygen concentration of boundary layer on the same horizontal plane. In sum, the simultaneous 3-D visualization of biofilm surface and biofilm oxygen distribution provides important information regarding the biofilm oxygen distribution near biofilm surface.

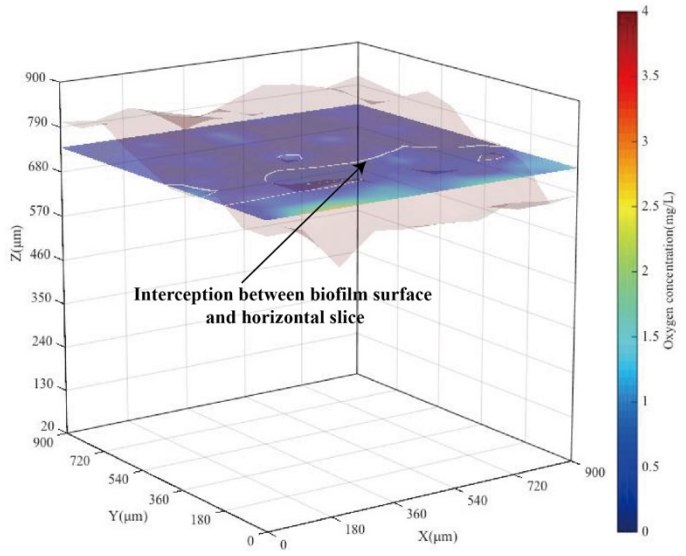

Fig 4-6 3-D visualization of oxygen distribution near biofilm surface

4.2.3 Animation

By copying, pasting and running the program in Appendix H at Matlab, the animated version of Fig 4-5 with a rotating perspective around z axis can be produced. By changing the arguments in line 55 of Appendix H and then running the program, another animated version of Fig 4-5 with a changing polar angle can be produced. Due to the crests and troughs of the biofilm surface, some details regarding the oxygen distribution on the biofilm surface were shielded in the static Fig 4-5. The animated versions of Fig 4-5 allow for the presentation of oxygen distribution information that are hard to be seen in the static figure. The animations will be as .avi files into Matlab folders, and is available at YouTube:

Animated version 1 of Fig 4-5: https://youtu.be/d0TvVXR6GGU

Animated version 2 of Fig 4-5: https://youtu.be/mMxRFatN93o

By copying, pasting and running the program in Appendix I at Matlab, the animated version of Fig 4-6 with can be produced. The animated Fig 4-6 has a rotating perspective around z axis and has a moving colormap slice from the lowest point to the highest point of biofilm surface. The change of interception between biofilm surface and horizontal slices can be clearly visualized in animated Fig 4-6. Similarly, the animated Fig 4-6 allows for the presentation of more details regarding 3-D oxygen distribution near biofilm surface compared with the visualization with static figure. The animation will be saved as .avi files into Matlab folders, and is available at YouTube:

Animated version of Fig 4-6: https://youtu.be/ejAaUnStM2M

5 Conclusions and recommendations

5.1 Conclusions

In this study, a Matlab package for effective 3-D visualization of oxygen distribution in wastewater biofilm as well as on and near biofilm surface was developed. The oxygen concentrations were measured by using oxygen microsensor in a previous study. The colormap slices, contour slices, isosurfaces, and animation were used for the visualization of 3-D oxygen heterogeneity. Only the basic module of Matlab commercial package and an ordinary desktop or laptop computer are required for running of Matlab package.

The 3-D visualization of oxygen distribution presented several interesting phenomena that could not be observed in the visualization of the previous study. The oxygen pockets in deep sections of biofilm were observed to exist in isolation, which indicates that the biofilm is physiologically heterogeneous. The oxygen concentration on the biofilm surface was observed to be much lower than that of bulk liquid phase, indicating a high intensity of metabolic activity in biofilm. The interception line between biofilm surface and horizontal slice was clearly visualized, which is helpful for comparing the vertical distribution of bacteria biovolume along the biofilm depth.

Since the 3-D profiles of other chemical species will be in the same form of the 3-D oxygen profile visualized in this study, the Matlab package in this study can also be used for the visualization of 3-D profiles of other chemical species (e.g. pH, redox potential, hydrogen sulfide, sulfate, methane, ammonium, nitrite, nitrate, chlorine, and monochloramine) measured by microsensors. The volume of visualization zone can be enlarged, and the number of individual profiles in the visualization zone can be increased. The visualization method presented in this study will greatly help researchers understand the 3-D

heterogeneity of biofilms, and to gain more insight for the structural and functional features of biofilms.

5.2 Recommendations for future research

Based the conclusions of the present study, I have two recommendations for future research:

(1) To our best knowledge, the 3-D oxygen profile measured by de la Rosa and Yu (2005) is the only published 3-D profile of chemical species inside biofilm. If the 3-D profiles of other chemical species are measured by other research groups using microsensors, it is recommended to visualize the new 3-D profiles for a better understanding of the structural and functional characteristics of biofilms.

(2) In Fig 4-6, the biofilm surface and oxygen distribution on a 740 μm horizontal plane is superimposed to present how oxygen distribution is relative to biofilm surface. However, the color of biofilm surface interferes with colors on the horizontal slice, making oxygen concentrations on the plane hard to be distinguished. Several color schemes were tested, and it was found that the color combination used in this study (brown for biofilm surface and jet colorbar for slice) leading to minimum interfering effect. Even so, the interfering effect cannot be eliminated. Thus, the development of a better strategy for explicitly visualizing oxygen distribution near biofilm surface is recommended for future research.

References

Allen, A., Habimana, O., & Casey, E. (2018). The effects of extrinsic factors on the structural and mechanical properties of Pseudomonas fluorescens biofilms: A combined study of nutrient concentrations and shear conditions. *Colloids and Surfaces B: Biointerfaces*, *165*, 127-134.

Bicubic interpolation. (n.d.). In *Wikipedia*. Retrieved from https://en.wikipedia.org/wiki/Bicubic_interpolation

Bishop, P. L. (1997). Biofilm structure and kinetics. *Water Science and Technology*, 36(1), 287-294.

Babauta, J. T., Nguyen, H. D., Istanbullu, O., & Beyenal, H. (2013). Microscale gradients of oxygen, hydrogen peroxide, and pH in freshwater cathodic biofilms. *Chemsuschem*, *6*(7), 1252-1261.

Beyenal, H., Donovan, C., Lewandowski, Z., & Harkin, G. (2004). Three-dimensional biofilm structure quantification. *Journal of Microbiological Methods*, *59*(3), 395-413.

Bridier, A., Dubois-Brissonnet, F., Boubetra, A., Thomas, V., & Briandet, R. (2010). The biofilm architecture of sixty opportunistic pathogens deciphered using a high throughput CLSM method. *Journal of Microbiological Methods*, *82*(1), 64-70.

De Beer, D., Stoodley, P., Roe, F., & Lewandowski, Z. (1994). Effects of biofilm structures on oxygen distribution and mass transport. *Biotechnology and Bioengineering*, 43(11), 1131-1138.

De Beer, D., Schramm, A., Santegoeds, C. M., & Kuhl, M. (1997). A nitrite microsensor

for profiling environmental biofilms. *Applied and Environmental Microbiology*, 63(3), 973-977.

De la Rosa, C., & Yu, T. (2005). Three-dimensional mapping of oxygen distribution in wastewater biofilms using an automation system and microelectrodes. *Environmental Science & Technology*, 39(14), 5196-5202.

Eberl, H. J., Picioreanu, C., Heijnen, J. J., & Van Loosdrecht, M. C. M. (2000). A three-dimensional numerical study on the correlation of spatial structure, hydrodynamic conditions, and mass transfer and conversion in biofilms. *Chemical Engineering Science*, 55(24), 6209-6222.

Fernández, C. E., Fontana, M., Samarian, D., Cury, J. A., Rickard, A. H., & González-Cabezas, C. (2016). Effect of fluoride-containing toothpastes on enamel demineralization and streptococcus mutans biofilm architecture. *Caries Research*, *50*(2), 151-158.

Jin, Y. L., Lee, W. N., Lee, C. H., Chang, I. S., Huang, X., & Swaminathan, T. (2006). Effect of DO concentration on biofilm structure and membrane filterability in submerged membrane bioreactor. *Water Research*, *40*(15), 2829-2836.

Kiamco, M. M., Atci, E., Mohamed, A., Call, D. R., & Beyenal, H. (2017). Hyperosmotic agents and antibiotics affect dissolved oxygen and pH concentration gradients in Staphylococcus aureus biofilms. *Applied and Environmental Microbiology*, AEM-02783.

Klug, B., Santigli, E., Westendorf, C., Tangl, S., Wimmer, G., & Grube, M. (2016). From mouth to model: combining in vivo and in vitro oral biofilm growth. *Frontiers in Microbiology*, *7*, 1448.

Harrison, J. J., Ceri, H., Yerly, J., Stremick, C. A., Hu, Y., Martinuzzi, R., & Turner, R. J.

(2006). The use of microscopy and three-dimensional visualization to evaluate the structure of microbial biofilms cultivated in the Calgary Biofilm Device. *Biological Procedures Online*, *8*(1), 194.

Habimana, O., Heffernan, R., & Casey, E. (2017). Nanofiltration-induced cell death: An integral perspective of early stage biofouling under permeate flux conditions. *Journal of Membrane Science*, *541*, 93-100.

Lawrence, J. R., Korber, D. R., Hoyle, B. D., Costerton, J. W., & Caldwell, D. E. (1991). Optical sectioning of microbial biofilms. *Journal of Bacteriology*, *173*(20), 6558-6567.

Lewandowski, Z., & Beyenal, H. (2013). *Fundamentals of biofilm research*. CRC press.

Liu, H., Tan, S., Sheng, Z., Liu, Y., & Yu, T. (2014). Bacterial community structure and activity of sulfate reducing bacteria in a membrane aerated biofilm analyzed by microsensor and molecular techniques. *Biotechnology and Bioengineering*, *111*(11), 2155-2162.

Lu, R., & Yu, T. (2002). A field study on oxygen penetration in wastewater biofilms. *Proceedings of the Water Environment Federation*, *2002*(15), 25-36.

Mathworks. (2018a, March 8). Interp3. *Matlab R2018a Documentation*. Retrived from: https://www.mathworks.com/help/matlab/ref/interp3.html

Mathworks. (2018b, March 8). Hold. *Matlab R2018a Documentation*. Retrived from: https://www.mathworks.com/help/matlab/ref/hold.html

Mathworks. (2018c, March 15). Slice. *Matlab R2018a Documentation*. Retrived from: https://www.mathworks.com/help/matlab/ref/slice.html

Mathworks. (2018d, March 15). Contourslice. *Matlab R2018a Documentation*. Retrived from: https://www.mathworks.com/help/matlab/ref/contourslice.html

Mathworks. (2018e, March 15). Isosurface. *Matlab R2018a Documentation*. Retrived from: https://www.mathworks.com/help/matlab/ref/isosurface.html

Mathworks. (2018f, March 29). Overview of volume visualization. *Matlab R2018a Documentation*. Retrived from: https://www.mathworks.com/help/matlab/visualize/overview-of-volume-visualization.html

Mathworks. (2018g, March 29). Lighting. *Matlab R2018a Documentation*. Retrived from: https://www.mathworks.com/help/matlab/ref/lighting.html

Montana State University Center for Biofilm Engineering. (2004, February 15). Biofilm structure simplified. Retrieved from: http://www.biofilm.montana.edu/multimedia/images/download.html?id=1096

Morgan, S. P., Rose, F. R., & Matcher, S. J. (2013). O*ptical Techniques in Regenerative Medicine*. CRC Press.

Morgenroth, E., Eberl, H., & van Loosdrecht, M. C. (2000a). Evaluating 3-D and 1-D mathematical models for mass transport in heterogeneous biofilms. *Water Science and Technology*, 41(4-5), 347-356.

Morgenroth, E., Van Loosdrecht, M. C. M., & Wanner, O. (2000b). Biofilm models for the practitioner. *Water Science and Technology*, *41*(4-5), 509-512.

Nakamura, S. (2002). *Numerical analysis and graphic visualization with MATLAB*. Upper

Saddle River, New Jersey: Prentice Hall PTR.

Nguyen, D., & Singh, P. K. (2006). Evolving stealth: genetic adaptation of Pseudomonas aeruginosa during cystic fibrosis infections. *Proceedings of the National Academy of Sciences*, *103*(22), 8305-8306.

Ning, Y. F., Chen, Y. P., Shen, Y., Zeng, N., Liu, S. Y., Guo, J. S., & Fang, F. (2014). A new approach for estimating aerobic–anaerobic biofilm structure in wastewater treatment via dissolved oxygen microdistribution. *Chemical Engineering Journal*, *255*, 171-177.

Noguera, D. R., Okabe, S., & Picioreanu, C. (1999). Biofilm modeling: present status and future directions. *Water Science and Technology*, 39(7), 273-278.

Pabst, B., Pitts, B., Lauchnor, E., & Stewart, P. S. (2016). Gel-entrapped Staphylococcus aureus as Models of Biofilm Infection Exhibit Growth in Dense Aggregates, Oxygen Limitation, Antibiotic Tolerance, and Heterogeneous Gene Expression. *Antimicrobial Agents and Chemotherapy*, AAC-01336.

Reihani, N., & Oddershede, L. B. (2009). Confocal microscopy of thick specimens. *Journal of Biomedical Optics*, 14(3), 030513.

Satoh, H., Sasaki, Y., Nakamura, Y., Okabe, S., & Suzuki, T. (2005). Use of microelectrodes to investigate the effects of 2-chlorophenol on microbial activities in biofilms. *Biotechnology and Bioengineering*, *91*(2), 133-138.

Staudt, C., Horn, H., Hempel, D. C., & Neu, T. R. (2004). Volumetric measurements of bacterial cells and extracellular polymeric substance glycoconjugates in biofilms. *Biotechnology and Bioengineering*, *88*(5), 585-592.

Stewart, P. S., & Franklin, M. J. (2008). Physiological heterogeneity in biofilms. *Nature Reviews Microbiology*, *6*(3), 199.

Tan, S., Yu, T., & Shi, H. C. (2014). Microsensor determination of multiple microbial processes in an oxygen-based membrane aerated biofilm. *Water Science and Technology*, *69*(5), 909-914.

Wang, J. H., Chen, Y. P., Dong, Y., Wang, X. X., Guo, J. S., Shen, Y., ... & Wang, J. (2017). A new method to measure and model dynamic oxygen microdistributions in moving biofilms. *Environmental Pollution*, *229*, 199-209.

Yu, T., & Bishop, P. L. (1998). Stratification of microbial metabolic processes and redox potential change in an aerobic biofilm studied using microelectrodes. *Water Science and Technology*, *37*(4-5), 195-198.

Zhang, T. C., & Bishop, P. L. (1995). Experimental determination of the dissolved oxygen boundary layer and mass transfer resistance near the fluid-biofilm interface. *Water Science and Technology*, 30(11), 47-58.

Zhou, X. H., Y, T., Shi, H. C., & Shi, H. M. (2011). Temporal and spatial inhibitory effects of zinc and copper on wastewater biofilms from oxygen concentration profiles determined by microelectrodes. *Water Research*, *45*(2), 953-959.

Zhou, X. H., Liu, J., Song, H. M., Qiu, Y. Q., & Shi, H. C. (2012). Estimation of heterotrophic biokinetic parameters in wastewater biofilms from oxygen concentration profiles by microelectrode. *Environmental Engineering Science*, *29*(6), 466-471.

Appendices: Matlab Programs

Appendix A: A Matlab program for generating colormap slices

```
clear, clc, close all
% Create a 3D mesh to contain oxygen data
[X1, Y1, Z1] = meshgrid(0:100:900, 0:100:900, 20:80:820);
% Import oxygen data
Oxygen(:, :, 1) = xlsread('Sample1.xls', 'layer1');
Oxygen(:, :, 2) = xlsread('Sample1.xls', 'layer2');
Oxygen(:, :, 3) = xlsread('Sample1.xls', 'layer3');
Oxygen(:, :, 4) = xlsread('Sample1.xls', 'layer4');
Oxygen(:, :, 5) = xlsread('Sample1.xls', 'layer5');
Oxygen(:, :, 6) = xlsread('Sample1.xls', 'layer6');
Oxygen(:, :, 7) = xlsread('Sample1.xls', 'layer7');
Oxygen(:, :, 8) = xlsread('Sample1.xls', 'layer8');
Oxygen(:, :, 9) = xlsread('Sample1.xls', 'layer9');
Oxygen(:, :, 10) = xlsread('Sample1.xls', 'layer10');
Oxygen(:, :, 11) = xlsread('Sample1.xls', 'layer11');
% Create a denser 3D mesh to contain oxygen interpolation
[X1i, Y1i, Z1i] = meshgrid(0:10:900, 0:10:900, 20:10:820);
% 3D interpolation with 'linear' method
Oxygen_i=interp3(X1,Y1,Z1,Oxygen,X1i,Y1i,Z1i,'linear')
% Create colormap slices and set properties of slices
x = [];
y = [];
z = [100 280 460 640 820];
h =slice(X1i, Y1i, Z1i, Oxygen_i, x, y, z)
set(h,'FaceColor','interp')
set(h,'EdgeColor','none')
% set box, axes, colors, and perspective
box on
grid on
axis([0 900 0 900 20 820]);
xlabel('X(μm)')
ylabel('Y(μm)')
zlabel('Z(μm)')
set(gcf,'position',[100 100 800 662])
```

```
35  set(gca, 'XTick', 0:180:900)
36  set(gca, 'YTick', 0:180:900)
37  set(gca, 'ZTick', 20:160:820)
38  set(gca, 'FontName', 'Times New Roman', 'FontSize', 14)
39  colormap jet
40  caxis([0, 4]);
41  colorbar
42  handl = colorbar;
43  set(handl, 'FontName', 'Times New Roman', 'FontSize', 14)
44  ylabel(handl, 'Oxygen concentration(mg/L)')
45  camproj perspective
46  view(-35, 15)
```

Appendix B: A Matlab program for generating contour slices

```
clear, clc, close all
% Create a 3D mesh to contain oxygen data
[X1, Y1, Z1] = meshgrid(0:100:900, 0:100:900, 20:80:820);
% Import oxygen data
Oxygen(:, :, 1) = xlsread('Sample1.xls', 'layer1');
Oxygen(:, :, 2) = xlsread('Sample1.xls', 'layer2');
Oxygen(:, :, 3) = xlsread('Sample1.xls', 'layer3');
Oxygen(:, :, 4) = xlsread('Sample1.xls', 'layer4');
Oxygen(:, :, 5) = xlsread('Sample1.xls', 'layer5');
Oxygen(:, :, 6) = xlsread('Sample1.xls', 'layer6');
Oxygen(:, :, 7) = xlsread('Sample1.xls', 'layer7');
Oxygen(:, :, 8) = xlsread('Sample1.xls', 'layer8');
Oxygen(:, :, 9) = xlsread('Sample1.xls', 'layer9');
Oxygen(:, :, 10) = xlsread('Sample1.xls', 'layer10');
Oxygen(:, :, 11) = xlsread('Sample1.xls', 'layer11');
% Create a denser 3D mesh to contain oxygen interpolation
[X1i, Y1i, Z1i] = meshgrid(0:10:900, 0:10:900, 20:10:820);
% 3D interpolation with 'linear' method
Oxygen_i=interp3(X1,Y1,Z1,Oxygen,X1i,Y1i,Z1i,'linear')
% Create the contourslices
x = []
y = [];
z = [300 640];
h =contourslice(X1i, Y1i, Z1i, Oxygen_i, x, y, z, 15)
% set box, axes, and perspective
box on
grid on
axis([0 900 0 900 20 820]);
xlabel('X(μm)')
ylabel('Y(μm)')
zlabel('Z(μm)')
set(gcf,'position',[100 100 800 662])
set(gca, 'XTick', 0:180:900)
set(gca, 'YTick', 0:180:900)
set(gca, 'ZTick', 20:160:820)
set(gca, 'FontName', 'Times New Roman', 'FontSize', 14)
colormap jet
```

```
colorbar
handl = colorbar;
set(handl, 'FontName', 'Times New Roman', 'FontSize', 14)
ylabel(handl, 'Oxygen concentration(mg/L)')
camproj perspective
view(-35, 25)
```

Appendix C: A Matlab program for generating isosurfaces

```
clear, clc, close all
% Create a 3D mesh to contain oxygen data
[X1, Y1, Z1] = meshgrid(0:100:900, 0:100:900, 20:80:820);
% Import oxygen data
Oxygen(:, :, 1) = xlsread('Sample1.xls', 'layer1');
Oxygen(:, :, 2) = xlsread('Sample1.xls', 'layer2');
Oxygen(:, :, 3) = xlsread('Sample1.xls', 'layer3');
Oxygen(:, :, 4) = xlsread('Sample1.xls', 'layer4');
Oxygen(:, :, 5) = xlsread('Sample1.xls', 'layer5');
Oxygen(:, :, 6) = xlsread('Sample1.xls', 'layer6');
Oxygen(:, :, 7) = xlsread('Sample1.xls', 'layer7');
Oxygen(:, :, 8) = xlsread('Sample1.xls', 'layer8');
Oxygen(:, :, 9) = xlsread('Sample1.xls', 'layer9');
Oxygen(:, :, 10) = xlsread('Sample1.xls', 'layer10');
Oxygen(:, :, 11) = xlsread('Sample1.xls', 'layer11');
% Create a denser 3D mesh to contain oxygen interpolation
[X1i, Y1i, Z1i] = meshgrid(0:10:900, 0:10:900, 20:10:820);
% 3D interpolation with 'linear' method
Oxygen_i=interp3(X1,Y1,Z1,Oxygen,X1i,Y1i,Z1i,'linear')
% create isosurfaces
p1= patch(isosurface(X1i,Y1i,Z1i,Oxygen_i,0.2));
isonormals(X1i,Y1i,Z1i,Oxygen_i,p1)
p1.FaceColor = 'blue';
p1.EdgeColor = 'none';
alpha(p1, 0.2)
p2= patch(isosurface(X1i,Y1i,Z1i,Oxygen_i,0.3));
isonormals(X1i,Y1i,Z1i,Oxygen_i,p2)
p2.FaceColor = 'green';
p2.EdgeColor = 'none';
alpha(p2, 0.2)
% set box, axes, perspective, colors and light
box on
grid on
axis([0 900 0 900 20 820]);
xlabel('X(μm)')
ylabel('Y(μm)')
zlabel('Z(μm)')
```

```
38  set(gcf,'position',[100 100 800 662])
39  set(gca, 'XTick', 0:180:900)
40  set(gca, 'YTick', 0:180:900)
41  set(gca, 'ZTick', 20:160:820)
42  set(gca, 'FontName', 'Times New Roman', 'FontSize', 14)
43  camproj perspective
44  view(-35, 15)
45  camlight
46  lighting gouraud
```

Appendix D: A Matlab program for generating 'colormap slices' animation

```
clear, clc, close all
% Create a 3D mesh to contain oxygen data
[X1, Y1, Z1] = meshgrid(0:100:900, 0:100:900, 20:80:820);
% Import oxygen data
Oxygen(:, :, 1) = xlsread('Sample1.xls', 'layer1');
Oxygen(:, :, 2) = xlsread('Sample1.xls', 'layer2');
Oxygen(:, :, 3) = xlsread('Sample1.xls', 'layer3');
Oxygen(:, :, 4) = xlsread('Sample1.xls', 'layer4');
Oxygen(:, :, 5) = xlsread('Sample1.xls', 'layer5');
Oxygen(:, :, 6) = xlsread('Sample1.xls', 'layer6');
Oxygen(:, :, 7) = xlsread('Sample1.xls', 'layer7');
Oxygen(:, :, 8) = xlsread('Sample1.xls', 'layer8');
Oxygen(:, :, 9) = xlsread('Sample1.xls', 'layer9');
Oxygen(:, :, 10) = xlsread('Sample1.xls', 'layer10');
Oxygen(:, :, 11) = xlsread('Sample1.xls', 'layer11');
% Create a denser 3D mesh to contain oxygen interpolation
[X1i, Y1i, Z1i] = meshgrid(0:10:900, 0:10:900, 20:10:820);
% 3D interpolation with 'linear' method
Oxygen_i=interp3(X1,Y1,Z1,Oxygen,X1i,Y1i,Z1i,'linear')
% Creation of animation
M = moviein(657);
for i =1:657
 h = slice(X1i, Y1i, Z1i, Oxygen_i, (i-1)*1.37, (i-1)*1.37, (i-1)*1.25);
 set(h,'FaceColor','interp')
 set(h,'EdgeColor','none')
 box on
 grid on
 axis([0 900 0 900 20 820]);
 xlabel('X(μm)')
 ylabel('Y(μm)')
 zlabel('Z(μm)')
 set(gcf,'position',[10 10 800 662])
 set(gca, 'XTick', 0:180:900)
 set(gca, 'YTick', 0:180:900)
 set(gca, 'ZTick', 20:160:820)
 set(gca, 'FontName', 'Times New Roman', 'FontSize', 14)
 colormap jet
```

```
caxis([0, 4]);
colorbar
handl = colorbar;
set(handl, 'FontName', 'Times New Roman', 'FontSize', 14)
ylabel(handl, 'Oxygen concentration(mg/L)')
title('3-D Oxygen Distribution in a Biofilm Sample Visualized by Colormap Slices')
axis vis3d
view(-55+i/4,15) % change the perspective
M(i) = getframe(gcf); % deliver all contents in the frame to animation
end
movie(M,1)
movie2avi(M,'Colormap slices.avi','compression', 'None','FPS',30)
```

Appendix E: A Matlab program for generating 'isosurfaces' animation

```
clear, clc, close all
% Create a 3D mesh to contain oxygen data
[X1, Y1, Z1] = meshgrid(0:100:900, 0:100:900, 20:80:820);
% Import oxygen data
Oxygen(:, :, 1) = xlsread('Sample1.xls', 'layer1');
Oxygen(:, :, 2) = xlsread('Sample1.xls', 'layer2');
Oxygen(:, :, 3) = xlsread('Sample1.xls', 'layer3');
Oxygen(:, :, 4) = xlsread('Sample1.xls', 'layer4');
Oxygen(:, :, 5) = xlsread('Sample1.xls', 'layer5');
Oxygen(:, :, 6) = xlsread('Sample1.xls', 'layer6');
Oxygen(:, :, 7) = xlsread('Sample1.xls', 'layer7');
Oxygen(:, :, 8) = xlsread('Sample1.xls', 'layer8');
Oxygen(:, :, 9) = xlsread('Sample1.xls', 'layer9');
Oxygen(:, :, 10) = xlsread('Sample1.xls', 'layer10');
Oxygen(:, :, 11) = xlsread('Sample1.xls', 'layer11');
% Create a denser 3D mesh to contain oxygen interpolation
[X1i, Y1i, Z1i] = meshgrid(0:10:900, 0:10:900, 20:10:820);
% 3D interpolation with 'linear' method
Oxygen_i=interp3(X1,Y1,Z1,Oxygen,X1i,Y1i,Z1i,'linear')
% create isosurfaces
p1= patch(isosurface(X1i,Y1i,Z1i,Oxygen_i,0.2));
isonormals(X1i,Y1i,Z1i,Oxygen_i,p1)
p1.FaceColor = 'blue';
p1.EdgeColor = 'none';
alpha(p1, 0.2)
p2= patch(isosurface(X1i,Y1i,Z1i,Oxygen_i,0.3));
isonormals(X1i,Y1i,Z1i,Oxygen_i,p2)
p2.FaceColor = 'green';
p2.EdgeColor = 'none';
alpha(p2, 0.2)
% set box, axes, perspective, colors and light
box on
grid on
axis([0 900 0 900 20 820]);
xlabel('X(μm)')
ylabel('Y(μm)')
zlabel('Z(μm)')
```

```
set(gcf,'position',[100 100 800 662])
set(gca, 'XTick', 0:180:900)
set(gca, 'YTick', 0:180:900)
set(gca, 'ZTick', 20:160:820)
set(gca, 'FontName', 'Times New Roman', 'FontSize', 14)
camproj perspective
view(-35, 15)
title('3-D Oxygen Distribution in a Biofilm Sample Visualized by Isosurfaces')
camlight
lighting gouraud
% create the animation
axis vis3d
M = moviein(720); % create a marix with 360 rows to save animation
for i = 1:720
 view(-55+i/4,15) % change the perspective
 M(:,i) = getframe(gcf); % deliver all contents in the frame to animation
end
movie(M,1) % play the movie for one time
movie2avi(M,'Isosurface.avi','compression', 'None','FPS',30) % save the movie into a .avi file
```

Appendix F: A Matlab program for visualizing oxygen on biofilm surface

```
clear, clc, close all
% Create a 3D mesh to contain oxygen data
[X1, Y1, Z1] = meshgrid(0:100:900, 0:100:900, 20:80:900);
% Import oxygen data
Oxygen(:, :, 1) = xlsread('Sample1.xls', 'layer1');
Oxygen(:, :, 2) = xlsread('Sample1.xls', 'layer2');
Oxygen(:, :, 3) = xlsread('Sample1.xls', 'layer3');
Oxygen(:, :, 4) = xlsread('Sample1.xls', 'layer4');
Oxygen(:, :, 5) = xlsread('Sample1.xls', 'layer5');
Oxygen(:, :, 6) = xlsread('Sample1.xls', 'layer6');
Oxygen(:, :, 7) = xlsread('Sample1.xls', 'layer7');
Oxygen(:, :, 8) = xlsread('Sample1.xls', 'layer8');
Oxygen(:, :, 9) = xlsread('Sample1.xls', 'layer9');
Oxygen(:, :, 10) = xlsread('Sample1.xls', 'layer10');
Oxygen(:, :, 11) = xlsread('Sample1.xls', 'layer11');
Oxygen(:, :, 12) = xlsread('Sample1.xls', 'layer12');
% Create a denser 3D mesh to contain oxygen interpolation
[X1i, Y1i, Z1i] = meshgrid(0:10:900, 0:10:900, 20:10:900 );
% 3D interpolation with 'linear' method
Oxygen_i = interp3(X1,Y1,Z1,Oxygen,X1i,Y1i,Z1i,'linear')
% Create a 2D mesh and import biofilm thickness data
[X2, Y2] = meshgrid(0:100:900, 0:100:900);
Thickness = xlsread('Sample1.xls', 'thickness');
% Create a denser 2D mesh and perform biofilm thickness interpolation
[X2i, Y2i] = meshgrid(0:10:900, 0:10:900);
Thickness_i = interp2(X2,Y2,Thickness,X2i,Y2i,'linear')
% Create the curved colormap slice and set property of the colormap slice
h = slice(X1i, Y1i, Z1i, Oxygen_i, X2i, Y2i, Thickness_i)
alpha(h, 0.5)
set(h,'FaceColor','interp')
set(h,'EdgeColor','none')
% set box, axes, colors, lighting and perspective
box on
grid on
axis([0 900 0 900 20 900]);
xlabel('X(μm)')
ylabel('Y(μm)')
```

```
38  zlabel('Z(μm)')
39  set(gcf,'position',[100 100 800 662])
40  set(gca, 'XTick', 0:180:900)
41  set(gca, 'YTick', 0:180:900)
42  set(gca, 'ZTick', 20:110:900)
43  set(gca, 'FontName', 'Times New Roman', 'FontSize', 14)
44  colormap jet
45  caxis([0, 4]);
46  colorbar
47  handl = colorbar;
48  set(handl, 'FontName', 'Times New Roman', 'FontSize', 14)
49  ylabel(handl, 'Oxygen concentration(mg/L)')
50  camproj perspective
51  view(-35, 15)
```

Appendix G: A Matlab program for visualizing oxygen near biofilm surface

```
clear, clc, close all
% Create a 3D mesh to contain oxygen data
[X1, Y1, Z1] = meshgrid(0:100:900, 0:100:900, 20:80:900);
% Import oxygen data
Oxygen(:, :, 1) = xlsread('Sample1.xls', 'layer1');
Oxygen(:, :, 2) = xlsread('Sample1.xls', 'layer2');
Oxygen(:, :, 3) = xlsread('Sample1.xls', 'layer3');
Oxygen(:, :, 4) = xlsread('Sample1.xls', 'layer4');
Oxygen(:, :, 5) = xlsread('Sample1.xls', 'layer5');
Oxygen(:, :, 6) = xlsread('Sample1.xls', 'layer6');
Oxygen(:, :, 7) = xlsread('Sample1.xls', 'layer7');
Oxygen(:, :, 8) = xlsread('Sample1.xls', 'layer8');
Oxygen(:, :, 9) = xlsread('Sample1.xls', 'layer9');
Oxygen(:, :, 10) = xlsread('Sample1.xls', 'layer10');
Oxygen(:, :, 11) = xlsread('Sample1.xls', 'layer11');
Oxygen(:, :, 12) = xlsread('Sample1.xls', 'layer12');
% Create a denser 3D mesh to contain oxygen interpolation
[X1i, Y1i, Z1i] = meshgrid(0:10:900, 0:10:900, 20:10:900 );
% 3D interpolation with 'linear' method
Oxygen_i = interp3(X1,Y1,Z1,Oxygen,X1i,Y1i,Z1i,'linear')
% Create a 2D mesh and import biofilm thickness data
[X2, Y2] = meshgrid(0:100:900, 0:100:900);
Thickness = xlsread('Sample1.xls', 'thickness');
% Create a denser 2D mesh and perform biofilm thickness interpolation
[X2i, Y2i] = meshgrid(0:10:900, 0:10:900);
Thickness_i = interp2(X2,Y2,Thickness,X2i,Y2i,'linear')
% Create the colormap slice and set property of the colormap slice
x = [];
y = [];
z = [740];
h1= slice(X1i, Y1i, Z1i, Oxygen_i, x, y, z), hold on
alpha(h1, 0.5)
set(h1,'FaceColor','interp')
set(h1,'EdgeColor','none')
% Create biofilm surface and set property of the biofilm surface
h2 = surf(X2i,Y2i,Thickness_i)
alpha(h2, 0.3)
```

```
set(h2,'EdgeColor','none')
hold off
% set box, axes, colors, lighting and perspective
box on
grid on
axis([0 900 0 900 20 900]);
xlabel('X(μm)')
ylabel('Y(μm)')
zlabel('Z(μm)')
set(gcf,'position',[10 10 800 662])
set(gca, 'XTick', 0:180:900)
set(gca, 'YTick', 0:180:900)
set(gca, 'ZTick', 20:110:900)
set(gca, 'FontName', 'Times New Roman', 'FontSize', 14)
colormap jet
caxis([0, 4]);
colorbar
handl = colorbar;
set(handl, 'FontName', 'Times New Roman', 'FontSize', 14)
ylabel(handl, 'Oxygen concentration(mg/L)')
camproj perspective
view(-35, 15)
camlight
lighting gouraud
```

Appendix H: A Matlab program for animating 'oxygen on biofilm surface'

```
clear, clc, close all
% Create a 3D mesh to contain oxygen data
[X1, Y1, Z1] = meshgrid(0:100:900, 0:100:900, 20:80:900);
% Import oxygen data
Oxygen(:, :, 1) = xlsread('Sample1.xls', 'layer1');
Oxygen(:, :, 2) = xlsread('Sample1.xls', 'layer2');
Oxygen(:, :, 3) = xlsread('Sample1.xls', 'layer3');
Oxygen(:, :, 4) = xlsread('Sample1.xls', 'layer4');
Oxygen(:, :, 5) = xlsread('Sample1.xls', 'layer5');
Oxygen(:, :, 6) = xlsread('Sample1.xls', 'layer6');
Oxygen(:, :, 7) = xlsread('Sample1.xls', 'layer7');
Oxygen(:, :, 8) = xlsread('Sample1.xls', 'layer8');
Oxygen(:, :, 9) = xlsread('Sample1.xls', 'layer9');
Oxygen(:, :, 10) = xlsread('Sample1.xls', 'layer10');
Oxygen(:, :, 11) = xlsread('Sample1.xls', 'layer11');
Oxygen(:, :, 12) = xlsread('Sample1.xls', 'layer12');
% Create a denser 3D mesh to contain oxygen interpolation
[X1i, Y1i, Z1i] = meshgrid(0:10:900, 0:10:900, 20:10:900 );
% 3D interpolation with 'linear' method
Oxygen_i = interp3(X1,Y1,Z1,Oxygen,X1i,Y1i,Z1i,'linear')
% Create a 2D mesh and import biofilm thickness data
[X2,Y2] = meshgrid(0:100:900, 0:100:900);
Thickness = xlsread('Sample1.xls', 'thickness');
% Create a denser 2D mesh and perform biofilm thickness interpolation
[X2i, Y2i] = meshgrid(0:10:900, 0:10:900);
Thickness_i = interp2(X2,Y2,Thickness,X2i,Y2i,'linear')
% Create the colormap slice and set property of the colormap slice
h = slice(X1i, Y1i, Z1i, Oxygen_i, X2i, Y2i, Thickness_i)
alpha(h, 0.5)
set(h,'FaceColor','interp')
set(h,'EdgeColor','none')
% set box and axes
box on
grid on
axis([0 900 0 900 20 900]);
xlabel('X(μm)')
ylabel('Y(μm)')
```

```
zlabel('Z(μm)')
set(gcf,'position',[100 100 800 720])
set(gca, 'XTick', 0:180:900)
set(gca, 'YTick', 0:180:900)
set(gca, 'ZTick', 20:110:900)
set(gca, 'FontName', 'Times New Roman', 'FontSize', 14)
colormap jet
caxis([0, 4]);
colorbar
handl = colorbar;
set(handl, 'FontName', 'Times New Roman', 'FontSize', 14)
ylabel(handl, 'Oxygen concentration(mg/L)')
title('3-D Oxygen Distribution on the Surface a Biofilm Sample')
% create the animation
axis vis3d
M = moviein(720); % create a marix with 360 rows to save animation
for i = 1:720,
 view(-55+i/4, 15) % change the perspective
 M(:,i) = getframe(gcf); % save each frame into the matrix M
end
movie(M,1) % play the movie for one time
movie2avi(M,'On the surface 1','compression', 'None','FPS',30) % save the movie into a .avi file
```

Appendix I: A Matlab program for animating 'oxygen near biofilm surface'

```
% Create a 3D mesh to contain oxygen data
[X1, Y1, Z1] = meshgrid(0:100:900, 0:100:900, 20:80:900);
% Import oxygen data
Oxygen(:, :, 1) = xlsread('Sample1.xls', 'layer1');
Oxygen(:, :, 2) = xlsread('Sample1.xls', 'layer2');
Oxygen(:, :, 3) = xlsread('Sample1.xls', 'layer3');
Oxygen(:, :, 4) = xlsread('Sample1.xls', 'layer4');
Oxygen(:, :, 5) = xlsread('Sample1.xls', 'layer5');
Oxygen(:, :, 6) = xlsread('Sample1.xls', 'layer6');
Oxygen(:, :, 7) = xlsread('Sample1.xls', 'layer7');
Oxygen(:, :, 8) = xlsread('Sample1.xls', 'layer8');
Oxygen(:, :, 9) = xlsread('Sample1.xls', 'layer9');
Oxygen(:, :, 10) = xlsread('Sample1.xls', 'layer10');
Oxygen(:, :, 11) = xlsread('Sample1.xls', 'layer11');
Oxygen(:, :, 12) = xlsread('Sample1.xls', 'layer12');
% Create a denser 3D mesh to contain oxygen interpolation
[X1i, Y1i, Z1i] = meshgrid(0:10:900, 0:10:900, 20:10:900 );
% 3D interpolation with 'linear' method
Oxygen_i = interp3(X1,Y1,Z1,Oxygen,X1i,Y1i,Z1i,'linear')
% Create a 2D mesh and import biofilm thickness data
[X2,Y2] = meshgrid(0:100:900, 0:100:900);
Thickness = xlsread('Sample1.xls', 'thickness');
% Create a denser 2D mesh and perform biofilm thickness interpolation
[X2i, Y2i] = meshgrid(0:10:900, 0:10:900);
Thickness_i = interp2(X2,Y2,Thickness,X2i,Y2i,'linear')
% Creation of animation
M=moviein(500);
for i =1:500
x = [];
y = [];
z = [i/2+600];
h1= slice(X1i, Y1i, Z1i, Oxygen_i, x, y, z), hold on % Create the moving colormap slice
alpha(h1, 0.5)
set(h1,'FaceColor','interp')
set(h1,'EdgeColor','none')
h2=surf(X2i,Y2i,Thickness_i) % Create biofilm surface
alpha(h2, 0.3)
```

```
set(h2,'EdgeColor','none')
hold off
% set box, axes, lighting and perspective
box on
grid on
axis([0 900 0 900 20 850]);
xlabel('X(μm)')
ylabel('Y(μm)')
zlabel('Z(μm)')
set(gcf,'position',[10 10 800 662])
set(gca, 'XTick', 0:180:900)
set(gca, 'YTick', 0:180:900)
set(gca, 'ZTick', 20:160:820)
set(gca, 'FontName', 'Times New Roman', 'FontSize', 14)
colormap jet
caxis([0, 4]);
colorbar
handl = colorbar;
set(handl, 'FontName', 'Times New Roman', 'FontSize', 14)
ylabel(handl, 'Oxygen concentration(mg/L)')
camlight
lighting gouraud
title('3-D Oxygen Distribution near the Surface of a Biofilm Sample')
axis vis3d
view(-55+i/4,15) % change the perspective
M(:,i)=getframe(gcf); % save each frame into the matrix M
end
movie(M,1) % play the movie for one time
movie2avi(M,'Near the surface.avi','compression', 'None','FPS',30) % save the movie into a .avi file
```